Master's thesis

NTNU
Norwegian University of Science and Technology
Faculty of Natural Sciences
Department of Materials Science and Engineering

Peder Ekerhovd

Digital Twin for composite materials

Long term properties of the matrix phase in Fiber Reinforced Polymers

Master's thesis in Materials Science and Engineering, TMM4960
Supervisor: Andreas Echtermeyer
May 2020

NTNU
Norwegian University of
Science and Technology

Peder Ekerhovd

Digital Twin for composite materials

Long term properties of the matrix phase in Fiber Reinforced Polymers

Master's thesis in Materials Science and Engineering, TMM4960
Supervisor: Andreas Echtermeyer
May 2020

Norwegian University of Science and Technology
Faculty of Natural Sciences
Department of Materials Science and Engineering

NTNU
Norwegian University of
Science and Technology

Abstract

A Digital Twin for calculating development of fatigue and creep damage due to uniaxial loads in polymer component was developed. The Digital Twin performed a quantitative analysis of the damage arising based on a history of loading, temperature and moisture level.

Creep was calculated based on linear viscoelastic theory. Fatigue cycles were extracted from a loading history using the Rainflow counting algorithm, and the damage from each cycle was calculated by shifting a reference S-N curve. Linear viscoelastic theory was used to adapt the reference S-N curve to other temperatures or moisture levels. Miner's damage rule was used to sum the damage of the individual fatigue cycles.

The Digital Twin's predictions were confirmed to be in line with its underlying theory by comparing it to a number of reference cases. Compared to available experimental data, the predictions of the Digital Twin were qualitatively and quantitatively correct except in the case of the polymer being saturated with moisture. In this case the fatigue strength was underestimated to a certain degree.

The Digital Twin's predictions were further investigated for a number of hypothetical cases including accidents, maintenance intervals, and gradually decreasing loads. It was also demonstrated how a Digital Twin approach can be used to extend component lifetime beyond its original design life, based on sensor data.

Sammendrag

En Digital Tvilling (Digital Twin) ble utviklet for å kalkulere skade fra kryp og utmatting på grunn av en-akset belastning i plastkomponenter. Den Digitale Tvillingen gjorde en kvantitativ analyse av skaden som oppstår på bakgrunn av historisk belastning, temperatur og fuktighetsnivå.

Kryp ble regnet ut basert på lineær viskoelastisk teori. Utmattingssykluser ble ekstrahert fra en belastningshistorie ved hjelp av Rainflow counting algoritmen. Skaden fra hver syklus ble regnet ut fra en referanse S-N kurve. Lineær viskoelastisk teori ble brukt for å tilpasse referansekurven til nye temperatur og fuktighetsnivåer. Miners skaderegel ble brukt for å summere skaden fra hver inviduelle syklus.

Det ble bekreftet at utregningene til Digitale Tvillingen stemte overens med den underliggende teorien ved å sammenligne de med ulike referansetilfeller. Utregningene tilden Digitale Tvillingen stemte overens med tilgjengelige eksperimentelle data, utenom utmattingsmotstanden for en polymer som var mettet med vann. I dette tilfellet ble utmattingsstyrken underestimert.

Den Digitale Tvillingen ble videre undersøkt for en rekke hypotetiske tilfeller, inkludert ulykker, vedlikeholdsintervaller og gradvis nedadgående belastninger. Det ble også demonstrert hvordan den Digitale Tvillingen kan bruks til å forlenge levetiden til komponenter, ved å bruke data innhentet fra sensorer.

Preface and Acknowledgement

The work presented in the following thesis was conducted the spring of 2020 at the Department of Mechanical and Industrial Engineering at the University of Science and Technology (NTNU). The project is a continuation of the specialization project written the fall of 2019. Sections 2.1, 2.2, 2.3, 2.4, 2.6, plus parts of Chapter 1 and Sections 2.5, 2.8, were adapted or lifted from the specialization project.

I would like to direct a special thank you to my supervisor, Prof. Andreas Echtenmeyer for all his help and expert guidance during the project. I would also like to thank Morten Johnsrud of Lundin Norway for giving me a technical project relevant to my thesis during my summer internship in the company, as well as my friend Eivind Meyer for his expert advice in *Python* and *Latex*.

I would also like to acknowledge the work of Dr. Andrey Krauklis and Dr. Abedin Gagani, whose research provided the experimental data that served as the foundation for the Digital Twin created during this Master thesis.

Table of Contents

List of Tables

List of Figures

Chapter 1

Introduction

1.1 Background

Polymers and polymer based composite materials are important materials, with large untapped potentials in areas such as transport and energy. In the offshore energy industry, they are considered enablers in hard to reach areas [1, 2]. This enabling is due to the fact that they are light, strong and immune to traditional corrosion mechanisms. The use of composite components may contribute to reduced project costs [3].

Lightness, strength and immunity to traditional corrosion mechanisms are the main properties that make composite materials attractive. Offshore applications expose components to harsh environmental factors. These include sea water, fluctuating temperatures, chemicals, UV radiation and more. A component in use at a subsea or offshore installation might be in use for over 25 years and needs to withstand these environmental factors without having its mechanical properties degraded to an unacceptable level [4].

There is still no fundamental understanding of the environmental degradation mechanisms in composites [5]. This issue is aggravated by several of the degradation mechanisms having a synergistic nature [1]. Although several of the individual processes are well understood, there is still no practical method to predict the composite's long term properties, giving results that are useful for practical applications. In an attempt to remedy this, Echtermeyer et al. proposed a new method for determining laminate level material properties of composites, based on the properties of the constituent materials (fiber, sizing/interface and matrix) [6].

The polymer matrix is an important constituent in Fiber Reinforced Polymer (FRP) materials, and several of the FRP materials' properties are dominated by the matrix. The fibers, especially if they are made of carbon, are relatively stable within normal operating parameters. The majority of the changes in long-term properties of composites are caused by microscopic changes in the matrix and matrix-fiber interface phases [5]. Understanding

the matrix' long-term properties is therefore fundamental to understanding the long-term behavior of the composite. Determining the properties of a pure polymer is also of value in its own regard, as polymers are in widespread use as construction materials.

A Digital Twin is a digital representation of the actual or potential properties of a physical entity or process. In this thesis, the concept of a Digital Twin was used where a polymer material's mechanical properties such as fatigue, creep and stress-strain behavior can be described at each point in time as a function of environmental factors and history of use, by considering the degradation and failure mechanisms for the polymer. The Digital Twin performs these calculations based on physical models for the polymer's mechanical behavior and degradation mechanisms.

1.2 Motivation

Due to inability to predict their long-term properties, extensive testing regiments are typically required to qualify a composite component or material for service. Such testing programs are described in the design codes/guidelines DNVGL-ST-C501 and DNVGL-ST-F1191[1], which are used in offshore oil and gas developments. These testing regiments have proved to be good enough for ensuring project specification compliance, but they can be very costly and time-consuming [4]. The high cost of testing has been an obstacle for more widespread deployment of composite components offshore and onshore [6].

Using a Digital Twin approach to leverage models for the long-term degradation of a polymer, one can reap several benefits:

- Simplified test program. Based on the underlying *Linear Viscoelastic* (LVE) theory, one can calculate material behavior for a range of loading types and environmental conditions, based on fewer and cheaper tests than what is normally required.
- When a composite material is qualified for use in accordance with the aforementioned DNV-GL design codes, it is qualified up to a certain temperature. The strength of the material at the maximum temperature it is qualified for will then be the rated strength of the material for any temperature below the maximum, even if the actual strength at lower temperatures is higher. This means that if we want to use a material rated for a service temperature up to 90° when the temperature is 40° , structural integrity calculations will be done with lower strength and faster degradation rate than the real values. This can lead to increased project costs.

  Using a Digital Twin approach, on the other hand, one can perform structural integrity calculations with a strength that is much closer to the material's true strength at the temperature it will be exposed to.
- Combining a Digital Twin with sensor data, one can monitor the condition of a component in real time if the sensors are connected to the *IoT* (Internet of Things). The sensor data will then be continuously be registered and transferred. The advantage

[1] Both available at the website of DNV GL

of this is that a less conservative approach can be used when calculating component lifetime. Typically, component lifetime is calculated by considering constant the worst-case service conditions, e.g. constant max temperature and load, which shortens the components lifetime.

A Digital Twin model can continuously model degradation/residual life as a function of the actual use history which will usually be less severe – prolonging the components lifespan. If we know the material properties at a given level of aging, we can replace components less frequently - reducing cost.

Being able to know the condition of component in real time may also reduce the amount of on-site inspection needed.

1.3 Scope of work

The scope of work in this thesis is divided into two parts:

- Develop code for a Digital Twin predicting creep and fatigue development in an Epoxy polymer, as a result of an arbitrary load and temperature/moisture history. The theoretical foundation which the Digital Twin bases its calculations on is LVE theory, as well as Rainflow counting and Palmgren Miners rule.
- Develop code for a Digital Twin predicting stress-strain behavior of an Epoxy polymer, within the area of viscoelastic validity. This was realized during the project thesis.

Both the behaviors shall be described as functions of temperature, moisture and history of use. The code shall be written in the programming language Python, which is a general-purpose programming language that is in widespread use in Academia and business [7]. Python has an *API* (Application programming interface) for important software such as *Abaqus*, which means that it supports cross-linking with these.

1.3.1 Structure of thesis

Chapter 2 will explain the physical models/mechanisms of long-term degradation of polymers, as well as other underlying theory. An explanation of the Digital Twin concept and its potential benefits in the oil and gas industry is also included in this chapter

Chapter 3 will explain how the physical models are implemented in the Digital Twin, so that the polymer's response to loading and environmental conditions can be calculated. This chapter will also explain a case study aimed to validate the predictions and showcase the potential of the Digital Twin.

Chapter 4 will show how the Digital Twin predicts creep and fatigue damage to develop for a range of loading and temperature/moisture scenarios.

Chapter 5 will discuss the results presented in Chapter 4, with a special focus on the reliability of the results, and a summary of the Digital Twin's potential benefits and drawbacks.

Chapter 6 will present the final conclusion of the thesis, as well as some suggestions for future research.

Chapter 2

Theory

2.1 Polymers

Polymers are large chain linked organic molecules, consisting of repeating sub-units. The *International Union of Pure and Applied Chemistry, IUPAC*, defines polymers as follows:

A polymer is a substance composed of macromolecules. A macromolecule is a molecule of high relative molecular mass, the structure of which essentially comprises the multiple repetition of units derived, actually or conceptually, from molecules of low relative molecular mass. [8]

Unlike the metals, polymers tend to form glasses or semi-crystalline solids, rather than crystals [9]. This glass forming nature of many polymers is the root cause of several of their unique properties, such as viscoelastic mechanical behaviour.

The consequence of the viscoelastic behaviour of the polymers is that their mechanical properties are highly dependent on parameters such as temperature, strain-rate, as well exposure time to chemical environment (water, organic solvents, oxygen). [10]

2.2 Composite materials

A composite material is a material consisting of two or more components (*constituents*) that are different on a scale higher than molecular [11, 10].

Fiber reinforced polymers are one of the most commonly used composite materials. They are usually made up of glass or carbon fibers embedded in a polymer resin, with a sizing applied to the fibers to secure adhesion between the fibers and the matrix. This arrangement is shown schematically in Figure 2.1.

Figure 2.1 Illustration of the different components/constituents in a FRP composite material

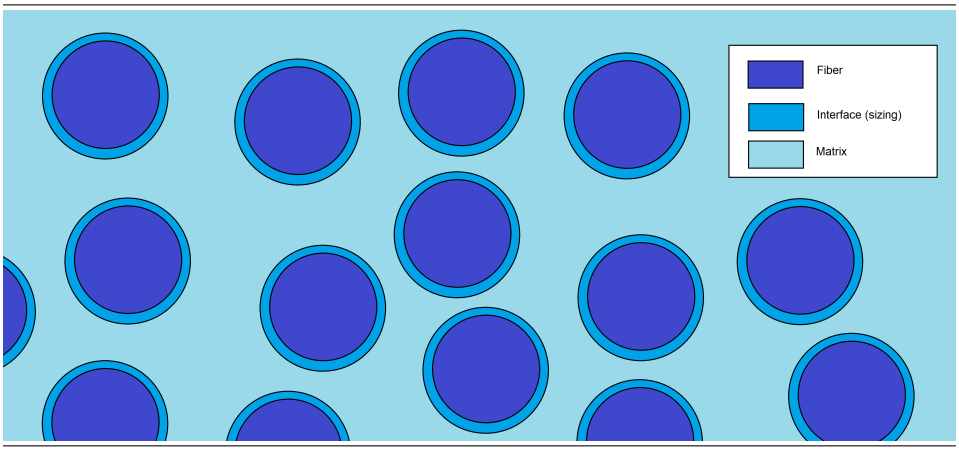

2.3 Degradation mechanisms in polymers and polymer based composite materials

Even tough polymers and polymer-based composites are not subject to traditional electrochemical degradation mechanisms such as corrosion, their properties will degrade over time due to factors such as mechanical loading, moisture, temperature fluctuations, UV-radiation and biological factors [12].

2.3.1 Liquid uptake in polymers and composite materials

A certain liquid uptake is unavoidable when polymers and composite components are exposed to humid environments. Water uptake in polymers is often termed *swelling*, due to an associated volume change.

Water molecules can diffuse both into the matrix, and into the sizing phase of a composite. Here, they will position themselves between the polymer chains, and increase the distance between them [13, 14]. Absorption of liquid will generally reduce the strength and stiffness of the polymer, while ductility and fracture toughness are increased. Since the fibers in FRP materials are more or less inert to water [15, 16], the water uptake affects mostly the matrix-dominated properties of composites, such as transverse and shear strength [5, 15].

Another effect of liquid uptake is that the glass-transition temperature, T_g, of the polymer is reduced. These effects are explained more in-depth in Section 2.6.1.

Note that even before exposure to water, a polymer will have a certain water content [17]. In this source, tensile tests were done on samples that had been saturated with water, before being re-dried. The re-dried specimen exhibited higher strength and elastic modulus as well as lower water content than the specimen that had not been exposed to water.

2.3.2 Reversible and irreversible degradation mechanisms

When a liquid diffuses into a polymer, it may in some cases cause chemical changes on the molecular level, termed *chemical degradation* [1, 12]. Chemical degradation includes effects such as chain scission (loss molecular weight), cross-link creation and hydrolysis. These are irreversible changes, which will affect the polymer even if the liquid is removed by a drying process.

If a liquid does not cause chemical changes in the matrix, the effects of swelling can be reversed, as shown in [17].

The implications of the reversible effects of liquid uptake, if the liquid do not cause chemical degradation, are explained in Section 2.6.1.

2.4 Multi-scale model of degradation in composites

The degradation mechanisms of FRP materials are complex, and this issue is aggregated by the wide range of FRP materials available. The fibers can have many configurations (woven, knitted, chopped, etc), while the matrix can be thermoset or thermoplastic. Data obtained for one system might therefore not be applicable if one or more parameters (Matrix type, fiber type and configuration) are changed. The diversity of the FRP material class might be a contributing factor in hindering the development of a comprehensive model for their long-term properties.

Composites will often exhibit a degradation profile through their thickness [1], with each individual ply being degraded to a different level. This means that even though some parts of the component, such as a pipe, are severely degraded (Ply in contact with transported fluid), the component might still perform its function (Collapse pressure of pipe is not significantly reduced).

Echtermeyer et al. presented a Multi-scale model for modelling the long-term properties of composite materials [6]. The model aims to use the properties of the constituent materials to predict the composite material's final properties on a ply/laminate level. The model can be summed up by the following steps:

1. Calculate moisture transport and crack/void development (for fatigue loading) in the composite. These will be functions of loading, chemical environment and temperature. One method for performing such calculations is proposed in [15].
2. Calculate how the combined effect of moisture, temperature and eventual crack development affect the material properties of each individual constituent material. This step will be the focus of the Digital Twin.
3. Calculate macro level (ply) material properties based on the properties of the constituents. This step is achived using micromechanics, and a representative volume element (RVE) method. Laminate level properties are determined using laminate theory, which is already a well established field.
4. The results obtained in step 3 can then be used as input in a FEA analysis, calculating

component residual lifetime or safety factor, based on its geometry, load situation and material properties.

The main benefits of this approach is that testing scope can be reduced. Ideally, material parameters for a wide range of temperatures and exposure times to moisture can be determined from a simplified/accelerated testing regime, where material properties are calculated rather than tested for each combination of operating parameters. This means one can calculate material properties for different exposure times and environmental conditions. These can serve as input in FEA calculations, such as for assessment of structural integrity or pressure containment capacity.

A somewhat similar approach was presented in [1]. Here it is described that in order to evaluate the long-term structural integrity of composite components, we need to know the degradation profile trough the material's thickness and material properties at a given level of aging (at ply level).

2.5 Linear Viscoelastic Theory

As explained in Section 2.1, polymers are viscoelastic materials.

Viscoelastic behaviour means that a material exhibits a mixture of elastic and viscous mechanical behaviour. This leads to a number of interesting properties, such as a time-dependency in their mechanical behaviour. These are explained in the following sections.

The linearity in linear viscoelasticity means that at a given time, for two loads that are qualitatively equal, the stress in each case is proportional to the strain and vice versa [18].

2.5.1 Stress-strain

Metals, when subject to strains less than 0.2%, exhibit an purely elastic stress-response when subject to strain, following Hook's law:

$$\sigma = E\varepsilon \tag{2.1}$$

E is the elastic modulus of the material, σ is the stress, and ε is the strain.

Polymers on the other hand, exhibit a mixture of elastic and viscous response when subjected to low strains. This mixed behaviour is expressed by a time dependency in the E-module, making Hook's law a function of time:

$$\sigma = E(t)\varepsilon \tag{2.2}$$

This behavior is modeled most simply by linear viscoelasticity, a field which is well-established. The mathematical foundation behind linear viscoelasticity has been studied for several decades [19]. The maximum strain limit for validity of pure linear viscoelastic $\sigma - \varepsilon$ behaviour is typically 1%. The exact limit depends on factors such as loading rate, moisture content and temperature [20]. For strains above the viscoelastic limit, non-linear

viscoelastic effects or plastic deformation can occur [21]. These effects will negate the validity of Linear Viscoelasticity.

Figure 2.2 shows a schematic comparison the elastic and the delayed viscoelastic response in response to the stress and strain histories shown on above each case.

Figure 2.2 Schematic illustrations of the elastic and viscoelastic behaviours in linear time, in response to constant applied stress or strain. Here, ε_0 is the elastic part of the viscoelastic strain

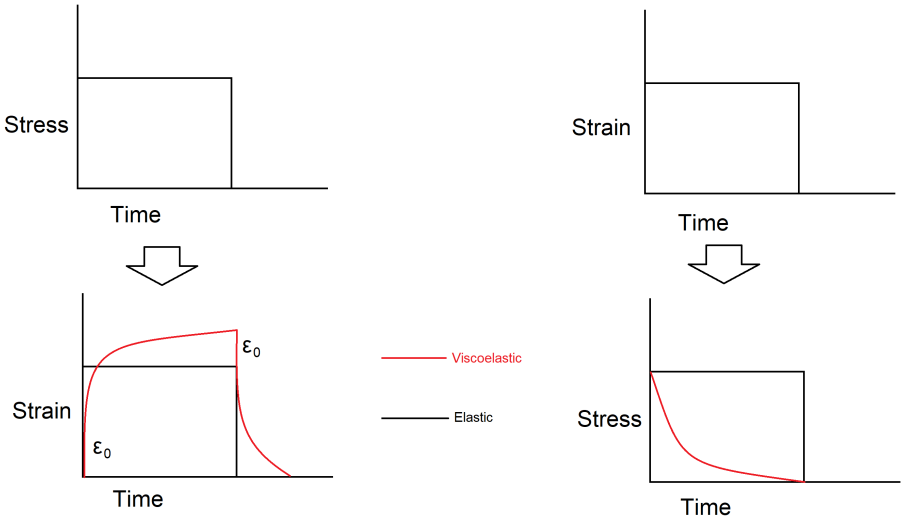

LVE is based on Boltzmann's super-position principle [22]. Boltzmann's super-position principle states that during loading, each step serves as an independent contribution to the final loading state. In short, this means that we can represent the time-dependent stress (σ) response, from a series of strain increments, of viscoelastic materials in the form of an integral:

$$\sigma(t) = \int_{-\infty}^{t} E_r(t-\tau)d\varepsilon(t) = \int_{-\infty}^{t} E_r(t-\tau)\frac{d\varepsilon}{d\tau}d\tau \tag{2.3}$$

Here, E_r(t) is the stress relaxation function, which is explained in Section 2.5.2. $\frac{d\varepsilon}{d\tau}$ is the strain rate, often written as $\dot{\varepsilon}$.

For the case of constant monotonic loading as explained in Equation (2.4), Equation (2.3) simplifies to Equation (2.5).

$$\varepsilon = \begin{cases} 0 & t < 0 \\ \dot{\varepsilon} \cdot t & t \geq 0 \end{cases} \tag{2.4}$$

$$\sigma(t) = \int_0^t E_r(t-\tau)\dot{\varepsilon}d\tau \tag{2.5}$$

Since the strain-rate is constant, the time-dependent stress in Equation 2.5 can easily be transformed strain-dependent stress, as shown below:

$$\sigma(\varepsilon) = \int_0^{\frac{\varepsilon}{\dot{\varepsilon}}} E_r(\frac{\varepsilon}{\dot{\varepsilon}} - \tau)\dot{\varepsilon}d\tau \tag{2.6}$$

2.5.2 Stress Relaxation

E_r(t), known as the stress relaxation function, is the viscoelastic stress response due to a constantly applied strain as a function of time, as shown on the right in Figure 2.2. Commonly, the stress relaxation function is written as an exponential series expansion, called a Prony Series [23]:

$$E_r(t) = g_0 + \sum_{i=1}^{N} g_i e^{-\frac{t}{\tau_i}} \tag{2.7}$$

Here N is the number of summands in the Prony Series. Typically, N≥5 is needed to accurately model the material's stress-relaxation behaviour over long time periods. The parameters τ_i and g_i are related to molecular-level interactions happening within the polymer when it is loaded. τ_i and g_i represent the characteristic time and the weight of each relaxation process, respectively. Figure 2.3 shows how τ_i and g_i relate to E_r(t) for the Prony Series given in Table 2.1.

N	g_i [MPa]	τ [s]
0	0.4	-
1	0.3	1e+01
2	0.3	1e+05

Table 2.1: Prony series of E_r in Figure 2.3

Equation 2.7 is equal to a generalized, multi-network Maxwell model, also known as Wiechert model, consisting of linear springs and Newtonian dashpots filled with viscous liquids, as shown in Figure 2.4 for N=3.

In Equation 2.7, g_0, and g_i, represent the spring constants, while the τ_i, the relaxation time, is related to the viscosity of the liquid inside each Newtonian dashpot.

Figure 2.3 Stress relaxation

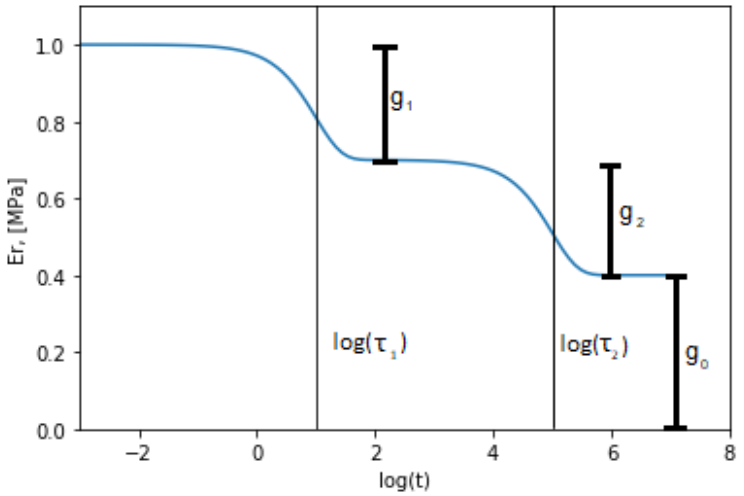

Figure 2.4 Multi-network generalized Maxwell model, N=3

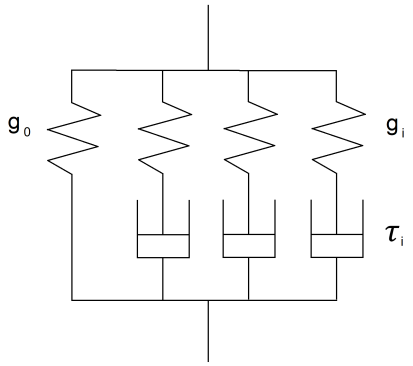

Prony series are employed in the widely used Finite Element Analysis (FEA) software *Abaqus*, and are generally considered to be very suitable for representing the $E_r(t)$-behaviour of polymers.

2.5.3 Creep

Creep is a material's time dependent strain-behaviour in response to applied stress, as shown schematically on the left in Figure 2.2. The creep strain consists of a elastic/instantaneous part, and a viscous/time dependent part. Creep behaviour is important for components that are subject to long-lasting stresses, especially if the temperature is high.

Creep is defined as follows:

$$\varepsilon_{creep}(t) = C(t) \cdot \sigma_0 \tag{2.8}$$

Here C(t) is the creep compliance function, and σ_0 is the applied stress . The elastic/instantaneous part of the creep is equal to $\sigma_0 \cdot C(0)$. The creep compliance is modelled by a Prony series similar to that of E_r:

$$C(t) = j_0 - \sum_{i=1}^{N} j_i e^{-\frac{t}{\lambda_i}} \tag{2.9}$$

Equation 2.9 is modeled by the Kelvin-Voigt model, which consists of linear springs and Newtonian dashpots, as shown in Figure 2.5 for N=3.

Figure 2.5 Kelvin-Voigt model for creep compliance

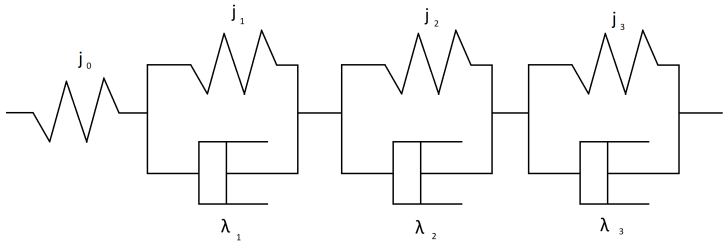

Figure 2.6 shows how λ_i, j_i relate to C(t), exemplified by the compliance Prony series given in Table 2.2.

N	j_i [1/MPa]	λ_i [s]
0	1	-
1	0.4	10
2	0.2	1e+4

Table 2.2: Prony series of C(t) in Figure 2.6

Following the same method as for stress-strain, the creep resulting from an arbitrary stress history can be calculated by Equation 2.10, which is the creep version of Equation 2.3:

$$\varepsilon(t) = \int_{-\infty}^{t} C(t-\tau)\frac{d\sigma}{d\tau}d\tau \tag{2.10}$$

2.6 Time-temperature Superposition

The stress relaxation and creep behavior of many polymers depend on the temperature. It has been shown experimentally that if the material is thermorheologically simple, the

Figure 2.6 Compliance curve and its relation to the Prony series parameters

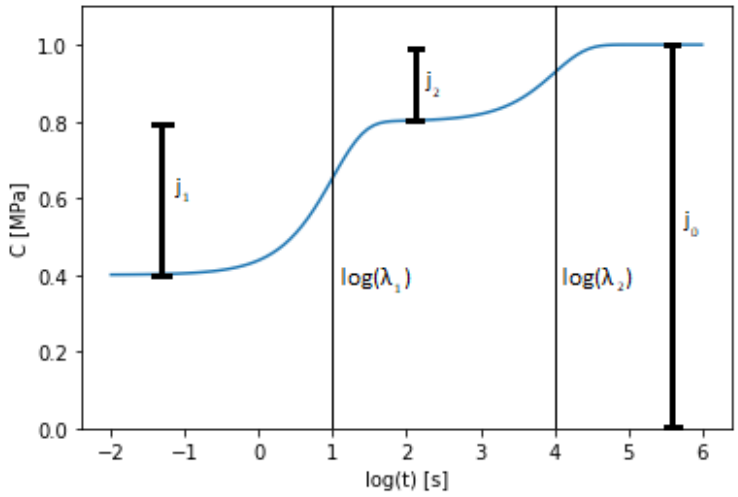

temperature-dependence can be modelled by a simple horizontal shift of the relaxation/creep function in logarithmic time scale [19]. Thermorheological simplicity means that every τ_i, λ_i is affected the same by any temperature change, ie $\tau_{i,T} = 10^{log(a)} \cdot \tau_{i,T_0}$.

The horizontal shift of $E_r(t)$ is shown schematically in Figure 2.7, where the curves T1, T2, T3 represents the E_r behaviour at different temperatures. The temperature of T1 is lower than that of T2 which is lower than that of T3.

Figure 2.7 Time-Temperature superposition of $E_r(t)$

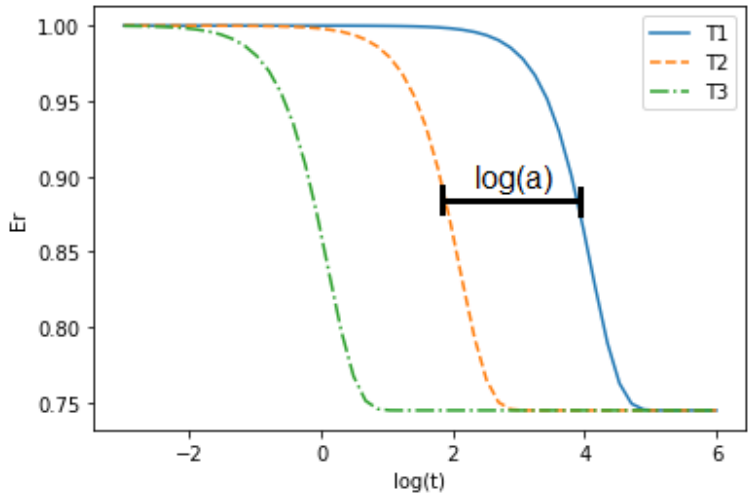

The implication of the Time-Temperature superposition principle is that a polymer's E_r(t) and C(t) behavior at higher or lower temperatures is the same as the behavior at a reference temperature, if the time was accelerated by a factor, a. In Figure 2.7, the absolute value of the acceleration factor between T2 and T3 is equal to 100, log(a) = 2. In this work, log represents the base 10 logarithm.

The acceleration, or shift factor, is defined as follows:

$$\begin{aligned} a_T &= \frac{t_T}{t_{T_0}} \\ log(a_T) &= log(t_T) - log(t_{T_0}) \end{aligned} \tag{2.11}$$

In Equation (2.11), t_{T_0} is the time at the reference temperature, T_0, while t_T is the equivalent time at another temperature, T_1. The shift factor can be calculated using Arrhenius approach:

$$log(a_T) = \frac{E_a}{2.303R}\left(\frac{1}{T_0} - \frac{1}{T}\right) \tag{2.12}$$

Here, E_a is the activation energy of the relaxation/creep process and R is the universal gas constant. Note that T and T_0 must be in Kelvin.

2.6.1 Time-Temperature-Plasticization superposition

Water uptake in polymers increases chain mobility and decreases the strength and modulus of the matrix and interface [15]. The increased chain mobility is normally attributed to an increase in the free volume of the polymer, which is the volume of the polymer that is not occupied by polymer chains. The increase of free volume is linked to an increase in chain mobility and a decrease in the glass transition temperature, T_g, of the polymer [21]. It has been shown that the shift in T_g influences E_r and C(t) in a similar way that an actual temperature shift does. This leads to the following equation:

$$log(a_{dry-wet}) = \frac{E_a}{2.303R}\left(\frac{1}{T_{g,dry}} - \frac{1}{T_{g,wet}}\right) \tag{2.13}$$

Here, $T_{g,dry}$ and $T_{g,dry}$, represent the glass transition temperature for the dry and wet polymer respectively.

The total logarithmic shift-factor resulting from a combination of temperature and moisture content is the sum of the shift factor due to moisture and the shift factor due to temperature change:

$$log(a_{tot}) = log(a_T) + log(a_{dry-wet}) \tag{2.14}$$

The acceleration factor is included into (2.5) by a accelerating the time, as follows:

$$\sigma(t) = \int_0^t E_r \left(10^{log(a_{tot})}(t-\tau)\right) \dot{\varepsilon} d\tau \tag{2.15}$$

The implication of the Time-Temperature-Plasticization principle is that if a liquid does not cause irreversible chemical degradation of the polymer, its influence on the polymer's mechanical properties can be modeled purely based on its influence on T_g. It has been shown [21] that Equation 2.13 was able to predict the shift of the compliance curve of a epoxy material reasonable well, but that for good quantitative agreement a experimental shift factor should be used.

2.7 Fatigue

Fatigue is the phenomena that causes a material to fail when subjected to cyclic loading, even if the loading induces a stress- or strain level far below the ultimate tensile or even yield strength of the material. It has been shown that fatigue damage can be incurred within the viscoelastic regiment [24]. Fatigue in polymers is generally believed to happen as a result of damage accumulation [25, 26], rather than the initiation and growth of a single crack as is the case for metals. Cyclic load damage in polymers can come as a result of both the fatigue element and creep element of the loading (creep damage is induced if the mean fluctuating load is non-zero).

Fatigue loading is usually characterized by two factors. In stress-controlled fatigue loading they are defined as S_a and S_m, which represents the amplitude (half the difference between maximum and minimum stress), and mean stress (average of maximum and minimum stress). R is defined as the minimum stress divided by the maximum.

Creep can be seen as the limiting case of fatigue when the loading amplitude goes towards 0, while the mean load is non-zero. Although increasing S_m has been shown to decrease fatigue life for a given stress amplitude S_a, predicting the exact relation between fatigue life and mean stress is a challenge that has not yet been fully solved.

2.7.1 Frequency effect

Fatigue in polymers has a frequency effect. Higher loading frequency typically increases number of cycles to failure [26]. There are several possible explanations for this effect. Although loading frequency has little impact on the cyclic creep rate, higher frequencies means shorter time to reach a certain number of cycles and thus less time for the cyclic creep to happen (less time per cycle equals less creep per cycle). Ultimately this reduces the creep's damaging effects. Another possible explanation is that the modulus and ultimate tensile strength of the polymer increases with loading frequency, which can be related to an increase in the strain rate. Since the frequency effect is thought to be related to creep damage, the frequency effect should expected to be more pronounced at higher R-ratios.

Note that in some experiments, the opposite effect is observed: fatigue life decreases with frequency. This is thought to be caused by heat build-up. Since the thermal conductivity of polymers is low, the hysteretic heat (heat generated by energy loss in hysteretic loop)

may for high frequencies not be dissipated rapidly enough, heating up the material and making it softer, and thus accelerating fatigue damage development.

2.7.2 Palmgren Miner's rule for cumulative damage

Often it is necessary to predict fatigue life of a component that is subject to several mean stresses or amplitudes. The most common method to predict fatigue failure in this case is called Palmgren Miner's rule [27], often termed Miner's rule. Miner's rule postulates that fatigue failure happens as a result of cumulative damage, and that the damage accumulation is linear with respect to number of cycles. This is represented by Equation 2.16.

$$M = \sum^{i} \frac{N_i}{N_{f,i}} \tag{2.16}$$

M is the Miner sum, which represents the cumulative damage. Failure by fatigue happens when M reaches unity. N_i is the number of cycles of a certain type (mean stress, amplitude, temperature, conditioning level), while $N_{f,i}$ is the number of cycles to failure for that type of cycle.

Miner's rule has been shown to work well for predicting fatigue life in isotropic materials, including polymers, subject to variable loading. This applies especially if the variable loading is random or periodical in nature. The main problem with Miner's rule is that it does not consider sequence effects, which are sometimes present. In metals, high-low load sequences may show failure for $M<1$, while low-high sequences may not show failure until $M > 1$.

2.7.3 Rainflow counting algorithm

Rainflow counting [28] is an algorithm used for fatigue analysis of loading data. The idea is to reduce a load history into a series of individual cycles whose impact can be calculated by Palmgren Miner's rule. The main characteristic of the method is that it treats lesser peaks and valleys in the load history as interruptions of the larger peaks and valleys.

Rainflow counting consists of four main steps, which are explained in short below:

1. Hysterisis filtering. This step aims to remove noise from the data. Noise is defined as cycles with a very small amplitude (the threshold amplitude is called the gate), which is thought to have little impact on the fatigue life.

2. Peak-valley filtering. In this step, all points that do not represent a reversak (peak or valley) in the stress history are removed.

3. Discretization. Here, each of the remaining points are rounded to the desired precision. Normally, the level of rounding is related to the amplitude gate used on Step 1.

4. Four-point counting method. Four consecutive peak/valley points are chosen: S1, S2, S3, S4. If |S1-S4| > |S2-S3| a cycle with amplitude |S2-S3| is counted and S2, S3 are removed.

The complete algorithm for Rainflow counting is described in *ASTM E1049 "Standard Practices for Cycle Counting in Fatigue Analysis"*.

2.7.4 Temperature and moisture effect

It have been shown that the effect of moisture uptake on fatigue strength of a polymer can be related to the moisture's effect on the ultimate tensile strength (UTS) of the material [17]. In this work it was assumed that the same was valid for the temperature's effect on UTS and fatigue strength. due to the temperature and moisture's similar effects on the creep curve of the polymer.

The new fatigue life is calculated by vertically shifting the S-N curve, based on the static strength reduction. The slope of the S-N curve is unchanged. The vertical shift between two hypothetical S-N curves, for dry and saturated epoxy where the liquid saturation causes the epoxy's UTS to decrease by 20%, is shown in Figure 2.8.

It was hypothesized that the reduction in UTS in percentage is close to the reduction at 1% strain. The latter can be predicted using LVE, thus providing a quick method to evaluate fatigue strength for different temperatures while reducing testing efforts.

Figure 2.8 Hypothetical S-N curves of saturated and dry epoxy

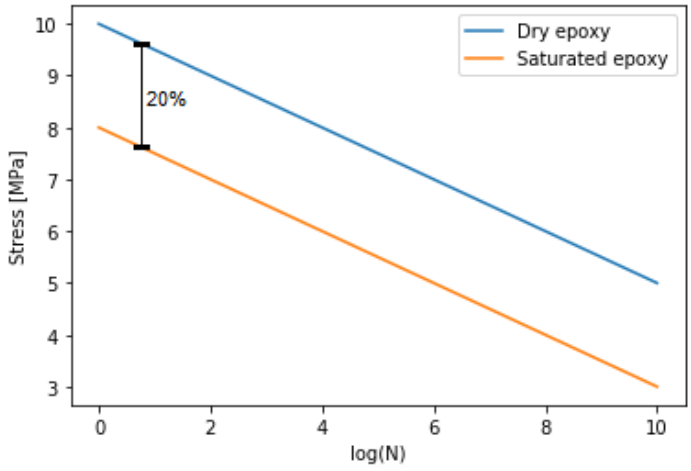

2.8 Digital Twin

2.8.1 Concept

In its broadest sense, a Digital Twin is a digital representation of a physical entity or process. At the time of the writing of this thesis, Digital Twin technology is an area of considerable ongoing research and industry interest. Different authors define Digital Twins differently [29, 30, 31].

Digital Twin technology in the oil and gas industry is of great interest, as it can provide great cost savings during the design and operational phase of a project. In the context of the oil and gas industry, one example of a Digital Twin for a pipeline system was defined by Bhowmik [32]. Here it was said that the Digital Twin acts as a digital replica of a field asset, which is monitored and maintained based on sensor data. In the work of Bhowmik, the Digital Twin is an integrated system, where sensors connected to the IoT gathers data, the data is analysed to draw insights which is then used in a preventative maintenance strategy.

The goal of a Digital Twin is to represent the actual or potential properties of its twin entity as accurately as possible. Digital Twins can serve a variety of purposes including performing real-time optimization of processes (such as preventative maintenance or calculating expected remaining useful life of a field asset), prediction of what-if/what-will cases during the design phase, and more. There are usually three key components in a Digital Twin: a set of analytics/algorithms, a data model, as well as data representative of the entity that is modeled.

In this thesis, the concept of a Digital Twin was used where the creep and fatigue behavior of a polymeric material could be described for a given load history/environmental parameters, by considering models for the physical degradation and failure in the polymer. Combining the Digital Twin for the polymer with an equivalent twin for the fiber and sizing phase, one could use the techniques explained in Section 2.4 to obtain a Digital Twin for the complete composite material/component.

2.8.2 Sensor integration

To calculate development of creep and fatigue in the polymer component, it is necessary to know the history of loads, temperatures, and moisture the component has been exposed to. The aforementioned information may be obtained by appropriate sensors. For the case of a polymer pipeline, pressure sensors/load cells, temperature sensors, as well as sensors detecting moisture/water immersion are needed.

In practice, creep strain can be measured directly by installing a strain gauge on the component, like how strain is measured in a tensile test. Nevertheless, being able to calculate creep based on a history of loads is valuable since it enables us to predict creep in the future based on assumed/expected loads and also benefits in interpreting the strain measured by the strain gauge. The measurements of the strain gauge can also be used to further refine the material parameters used by the Digital Twin, so that it can make better predictions for the future.

2.8.3 Application areas and potential benefits of the Digital Twin approach

A Digital Twin approach with sensor integration, as presented above, has many potential application areas. These can give benefits that can not be achieved by using only the underlying degradation models themselves:

- Monitor the material's properties/component status as a function of actual use conditions in real-time. Knowing material's condition in real time reduces the need for on-site inspections. Note that it is also possible to store the sensor data locally and retrieve them periodically if an online connection is found unfeasible.
- Calculate residual life based on history of use. Calculating residual life based on actual operation history has the potential to extend the lifespan of structures, since the actual usage will usually be less severe than the worst-case scenario typically used in the design phase to find the minimum lifetime.

  To evaluate service life the following is required: Service logs of loads, temperatures, and other relevant parameters, as well as knowledge of what impact these have on the properties of the material. The latter is calculated by the Digital Twin by considering physical degradation models.
- Digital Twin technology enables many scenarios to be examined in a short time. This can be leveraged to enable machine learning/reinforcement learning algorithms. If the Digital Twin for material properties is combined with Digital Twin for other parts of the oil and gas production infrastructure, machine learning can be used by the owner of a facility to find optimum operating parameters in order to maximize value by balancing production volume and maintenance intervals against component cost/lifetime/reliability.

Chapter 3

Method

3.1 Overview

In the previous section, the underlying theory and the degradation mechanisms considered by the Digital Twin were explained. In this section, it is demonstrated how these mechanisms are implemented in the Digital Twin.

An arbitrary load history may induce both fatigue and creep damage. The extent of which each damage mechanism is actually incurred depends on the fluctuations and mean of the load. In order to assess the integrity of the component, both the fatigue and creep part of damage must be evaluated. The extent of damage caused by a specific loading depends on temperature and conditioning level. The creep-rate is higher, and each fatigue cycle will cause more damage if the temperature is high and the polymer is saturated with liquid, compared to the damage at lower temperature and a dry polymer. This must be accounted for by the Digital Twin.

Although fatigue and creep damage are related, they were treated separately in this work due to a lack of methodology to comprehensively model the combined effect of creep and fatigue damage. For fatigue and creep, we define two different failure criteria. Failure is assumed to happen independently when either the Miner sum or creep strain reaches the failure criteria.

By using as input corresponding stress-time-temperature-conditioning data obtained from sensors installed on a component, one can use the Digital Twin to estimate the component's current condition. By appending hypothetical future data to the historical data, one can predict the remaining life of the component in different scenarios. One can also use entirely assumed data during the design phase of a component. In many cases, such as for an oil production pipeline, the relevant use data will be correlated to factors like production rate and weather conditions.

Relevant material parameters for the epoxy, limited to experimental acceleration factor for creep compliance due to moisture saturation, $\log(a)_{dry-wet}$=3.74, activation energy for creep, E_a=277 kJ/mol [1], creep data for fitting the Prony series of the epoxy's compliance plus reference experimental S-N data and UTS for dry epoxy, were taken from previous work [21, 17]. The fitting of the Prony series for creep compliance, and the interconversion to the stress relaxation series, were done during the specialization project. Since the aforementioned parameters are material specific, they properties must be re-tested if the Digital Twin shall be used for other polymeric materials other than the epoxy.

In Figure 3.1 a flow sheet is shown that summarizes how the complete Digital Twin works. The approach used in each step will be described in further detain in the following section.

Figure 3.1 Conceptual flowchart of the Digital Twin. The scope of work of this thesis is marked in red

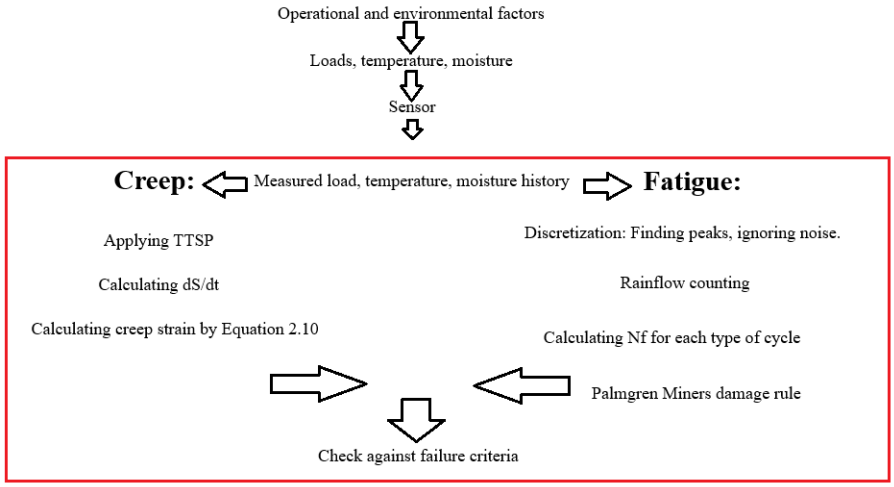

3.2 Creep

As explained in Section 2.5, creep-rate depends on stress level, temperature, and moisture. The effect of varying stress levels is inherently considered by Equation 2.10. To account for the effect of temperature and moisture, the TTSP-principle can be used. Typically, the TTSP-principle is used to compare viscoelastic behaviors at constant temperatures. In this work, the following methodology was used to consider the effect of varying temperature:

A given Time-Stress-Temperature history is converted to an equivalent Time-Stress history at constant temperature. Creep behavior at higher temperature, is equal to that of lower temperature if the time was accelerated by a factor $10^{log(a)}$. This means that we can model the effect of temperature changes by expanding time sections where the temperature was

[1] It was assumed that $\log(a)_{dry-wet}$ and E_a were equal for $E_r(t)$ and C(t)

higher than a reference temperature and contracting the time sections where the temperature was lower than the reference temperature by a factor of $10^{log(a)}$, where log(a) will be negative in the latter case.

In the code, a Time-Stress-Temperature history is converted to an equivalent Time-Stress constant temperature history, where the temperature is equal to the temperature for which the Prony series for creep compliance is valid. This is shown schematically in Figure 3.2, where the Prony series is normalized to the temperature at t=0s:

Figure 3.2 Schematic illustration of the Digital Twin's implementation of TTSP in the linear time domain

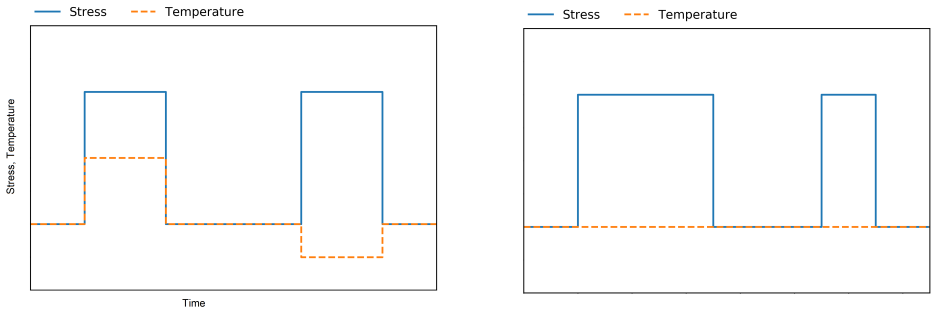

As seen in Figure 3.2 the stress-time sections exposed to higher temperatures are effectively expanded, while the ones exposed to lower temperatures are contracted. The two use histories will result in the same level of creep. The same principle can be used for time-moisture superposition since moisture uptake has the same effect as temperature increase. In practice, this is done as shown in Algorithm 1 (Pseudocode).

In Algorithm 1, T_r is the temperature that the Prony series for creep is normalized to. Tlist is the temperature history in list form, while tlist is the corresponding times. The output, tlistAdjusted, is the new list of times, as if the temperature was T_r the entire time. Note that algorithm 1 was given for temperature only. To account for the effect of moisture, the procedure is repeated, replacing Tlist with a list of the conditioning levels associated with each time. Note that the Twin only considers the extremes of moisture content: fully dry or fully saturated with liquid.

In order to evaluate Equation 2.10 to find the total strain, the trapeze method was used. When using the Digital Twin, the stress-time history will be available as discrete points due to the nature of the sensor. The continuous stress-time history was assumed to be the linear interpolation between each data point from the sensors installed on the component. This means that the slope of the stress-time history was assumed to be constant between each data point, as shown in Figure 3.3.

Increased sampling rate of the sensors will give a more accurate representation of the stress experienced by the component, which can make the predictions of the Digital Twin more accurate. The downside of increased sampling rate is the increased storage, connection bandwidth (if the component is monitored in real time) and computational efforts required.

Algorithm 1 TTSP Algorithm

Input: T_r, Tlist, tlist
Output: tlistAdjusted

tlistAdjusted = copy(tlist)
for i in range(length(tlist)) **do**
  T = Tlist[i]
  t = tlist[i]
  loga = $\frac{Ea}{2.303 \cdot 8.314} \cdot \left(\frac{1}{T_r} - \frac{1}{T}\right)$
  T_r = T
  tDiffs = [x-t for x in tlist]
  for j in range(length(tDiffs)) **do**
    if tDiffs[i] > 0 **then**
      tlistAdjusted[j] = t + tDiffs[i]$\cdot 10^{loga}$
    end if
  end for
end for

Figure 3.3 Sensor data points (sampling rate of 1/s) and linear interpolation, resulting in constant dS/dt (dτ/dt) between each data point.

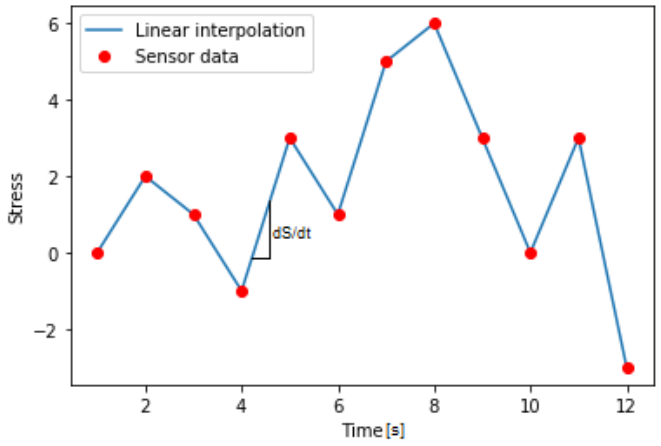

The required sampling rate depends on the frequency of the loading on the component. For higher frequencies, higher sample rate is needed. Typically, it is desired to have ten data points per cycle, which means that the sampling frequency needs to be at least ten times the highest loading frequency.

Algorithm 2 shows how Equation 2.10 is solved in Python. Slist and tlist is the list of stresses and corresponding times (adjusted to constant temperature), respectively. The output variable creep is the resulting creep.

Algorithm 2 Creep integral algorithm

Input: tlist, Slist
Output: creep

dSdt = $\frac{diff(Slist)}{diff(tlist)}$
tmax = tlist[-1]
creep = 0
for i in range(length(tlist)) **do**
  timeStep = tlist[j]
  Jstep = $J_0 - \sum^i j_i \cdot e^{\frac{-(tMax - timeStep)}{\lambda_i}}$
  creepStep = (tlist[j+1]-tlist[j]) ·dSdt[j]·Jstep
  creep = creep+creepStep
end for

3.3 Fatigue

3.3.1 Method outline

In order to evaluate fatigue damage resulting from an arbitrary stress-time-temperature history using conventional methods, the stress-time-temperature-moisture history must be reduced to a series of individual cycles. A popular method to extract cycles from a stress-time history is the Rainflow counting algorithm, which was described in Section 2.7.3. Applying the Rainflow counting method to a stress history obtained from sensors has earlier been explored for composite components in a windmill [33]. The DNVGL-ST-C501 standard states that Rainflow counting shall be used to establish fatigue history from a loading sequence, the fatigue history consisting of the number of cycles at each stress amplitude/mean combination.

Since even small temperature changes may have a strong influence on fatigue life in polymers, each fatigue cycle must also be associated with the temperature and conditioning level at which the cycle occurred. This means that in the Digital Twin the Rainflow algorithm must be modified so to also record the temperature and conditioning level associated with each cycle.

To apply the Rainflow counting algorithm, the stress-time-temperature history must be reduced to a series of local extreme points. This step is often termed discretization, and typically includes a gate (minimum prominence of extreme points), and a binning procedure. Binning means that each extreme point is rounded up or down. After discretization and binning, the Rainflow counting algorithm was performed, recording the cycles and their associated temperature/conditioning level. By using the Rainflow counting and associating each stress reversal with its corresponding temperature/conditioning level, the stress-temperature-conditioning-time history was reduced to number of cycles at each stress amplitude, mean, temperature and conditioning level. For each cycle, the following information was recorded:

N - Number of cycles

S_m – Stress mean

S_a – Stress amplitude

T – Temperature

C_{H_2O} – Conditioning level

In some cases, T and C_{H_2O} can vary during a cycle. In these cases, the maximum temperature and conditioning level of the cycle's starting and ending point were assumed to be valid for the entire cycle. Since changes in temperature and conditioning are usually slow compared to the duration of a cycle, this was deemed acceptable as a conservative approximation.

For each of the N-S_m-S_a-T-C_{H_2O} combinations, number of cycles to failure, N_f, was calculated, and N/N_f represents each combination's contribution to the Miner sum. N/N_f for each combination was summed, in order to find the Miner's sum at the end of the stress history.

3.3.2 Discretization/hysteresis filtering

In this work, the local extreme points were found using the *Python scipy.signal* package *find_peaks*. The *find_peaks* package includes the parameter *prominence*, which is equivalent to the gating/hysteresis filtering described in Section 2.7.3. The local maxima were found first by applying *find_peaks* to the stress-history, and subsequently the local minima by applying *find_peaks* to the negative stress-time history. To create the complete list of turning points, the list of local maxima and minima were interweaved. To achieve the effect of binning, each element in the list of turning points was rounded to the desired precision.

3.3.3 Four point counting

The 4-point counting was performed by a slightly modified version of a publicly available implementation [34]. A modification was done by also having as input two lists containing the temperature and conditioning level associated with each stress reversal. The cycle counting was based on the list of stress reversals, but when a cycle was found, the equivalent elements in the temperature and conditioning lists were also recorded. This created a 2D matrix, where each column gives information about a single/half cycle.

3.3.4 Calculating fatigue life at given stress levels and conditions

Calculating the effect of stress level

For the given epoxy material, it has been shown that the fatigue life can be predicted by Equation 3.1 for R=0.1 [17]:

$$log(N_f) = A \cdot log(S_{max}) + B \tag{3.1}$$

Here S_{max} is the maximum stress, which is equal to $\frac{S_a}{0.45}$ for R=0.1. A and B are material constants which can be found by performing least square fitting on S-N test data. To calculate N_f for other values of R, one must consider the mean-stress effect. The Smith-Watson-Topper-method (SWT) has been shown to work relatively well for polymeric materials [35]. The SWT-method, unlike the Goodman diagram which is typically used, does not require the yield strength or UTS of the material to be known. This is an advantage when calculating the mean stress effect in polymers, since the yield strength and UTS can vary significantly due to temperature and moisture.

Equation 3.2 shows how a combination of mean stress and amplitude is converted to an equivalent amplitude at zero mean stress, $S_{a,R=-1}$, in the SWT-method.

$$S_{a,R=-1} = \sqrt{S_a \cdot (S_a + S_m)} \tag{3.2}$$

Since the S-N curve was given for R=0.1, it was decided to perform the mean stress correction by a two-step procedure. First, the original (S_a, S_m) from the Rainflow counting was converted into $S_{a,R=-1}$ by Equation 3.2 (R=-1 corresponds to S_m=0). Then, $S_{a,R=-1}$ was converted into $S_{a,R=0.1}$ by Equation 3.3.

$$S_{a,R=0.1} = \sqrt{\frac{9}{20}} \cdot S_{a,R=-1} \tag{3.3}$$

Equation 3.3 was found as follows: For R=0.1, $S_m = 9/11 \cdot S_a$. Inserting this into Equation 3.2, and solving for S_a one obtains Equation 3.3. $S_{a,R=0.1}$ can then be inserted into Equation 3.1, where $S_{max} = \frac{S_{a,R=0.1}}{0.45}$.

Calculating the temperature and moisture effect

For polymeric materials, chain scission is the primary fatigue degradation mechanism [5]. It has further been suggested that the rate of this process is accelerated by higher temperatures and the presence of moisture. Two possible methods to account for this effect are presented below:

- It has been shown that decrease in stress amplitude at a given N_f due to a temperature increase is approximately the same as the decrease in static strength, which leads to the relationship shown in Equation 3.4. This means one can do a vertical shift of the S-N curve, to find fatigue life at other temperatures and conditioning levels than what was originally tested. This is the method that was used by the Digital Twin.

$$\frac{\sigma}{\sigma_r} = \frac{S_a}{S_{a,r}} \tag{3.4}$$

Here, σ is the static strength at $\varepsilon = 1\%$, $\dot{\varepsilon}$=0.00014/s [2], for the conditions (T, C_{H_2O}) one wishes to find the fatigue strength at, while σ_r is the static strength for an equivalent reference test at a known temperature and conditioning level. S_a is the fatigue strength at the actual conditions for a given N_f, while $S_{a,r}$ is the fatigue strength at N_f at the same conditions as the reference static test.

Calculating $\sigma(\varepsilon, \dot{\varepsilon}, T, C_{H_2O})$ for $\varepsilon = 1\%$ was done by Equation 2.15. This was explored in depth in the preparatory project for this thesis.

In order to take the temperature/moisture effect into account in Equation 3.1, one must modify the B obtained from the reference conditions (conditions of the S-N testing). To do this, one can use Equation 3.5.

$$B = -A_r \cdot log\left(\frac{\sigma}{\sigma_r}\right) + B_r \tag{3.5}$$

Here B_r and A_r are the obtained constants for the reference temperature and conditioning level. Note that A_r is not changed for use in Equation 3.1, since the slope of the S-N curve us unchanged.

- An alternative method would be to use Arrhenius approach directly. One such approach was presented in [5]. The idea here is that number of cycles is linearly dependent on time when the loading frequency is constant, which leads to Equation 3.6.

$$a = \frac{t}{t_r} = \frac{N_f}{N_{f,r}} \tag{3.6}$$

Here, t and N_f is the time and number of cycles to failure respectively, while t_r and N_r is the time and number of cycles to failure at the reference conditions. Under these assumptions, the number of cycles to failure at a given temperature can be modelled Equation 3.7, if there is no change in failure mechanism. Equation 3.7 can also be extended to include the effect of liquid saturation.

$$log(N) - log(N_r) = log(a) = \frac{-\Delta H}{2.303R}\left(\frac{1}{T_r} - \frac{1}{T}\right) \tag{3.7}$$

[2] $\dot{\varepsilon}$ was chosen on the basis of available $\sigma - \varepsilon$ experimental data for the reference curve, and ε = 1% is the approximate limit for validity of LVE

ΔH is the activation energy of the chain scission process.

A weakness of both methods is that it has not been tested experimentally if the shift factor is the same at different loading frequencies. Another weakness of the first method is that it has not been tested whether or not Palmgren Miner's rule is valid for calculating total number of cycles to failure when the temperature varies.

Frequency effect

The Digital Twin is that it did not consider the frequency effect when calculating the fatigue life, but in the typical range of frequencies encountered in field use the frequency effect is generally found to be relatively small.

3.3.5 Pseudocode

A simplified pseudocode for how fatigue is calculated by the Digital Twin is shown below. Algorithms 3 and 4 shows how $\sigma(\varepsilon, \dot{\varepsilon}, T, C_{H_2O})$ is calculated. Algorithm 5 shows how the Miner sum, M, is calculated from a stress history with corresponding temperatures, Slist, Tlist respectively. The effect of liquid saturation is calculated as for temperature, but is for readability purposes not shown in the pseudocode.

Algorithm 3 Integrand

Input: τ, t_{max}, log(a), E_0, g_i, τ_g
Output: σ

$\sigma = E_0 + \sum^i g_i \cdot e^{-10^{log(a)} \frac{(t_{max} - \tau)}{\tau_i}}$

Algorithm 4 stressLVE. Calculating σ at given ε. Constant strain rate, $\dot{\varepsilon}$

Input: ε, $\dot{\varepsilon}$, log(a), E_0, g_i, τ_g
Output: σ

$t_{max} = \frac{\varepsilon}{\dot{\varepsilon}}$

$\sigma = \dot{\varepsilon} \cdot \int_0^{t_{max}}$ Integrand(Integration variable = τ. Arguments = t_{max}, log(a), E_0, g_i, τ_g)

Algorithm 5 Calculating Miner sum, M, from a stress-temperature history

Input: Slist, Tlist
Output: M
peaks = find_peaks(Slist)
valleys = find_peaks(-Slist)
extremalsS = Slist[peaks, valleys]
extremalsT = Tlist[peaks, valleys]
fatigueHistory = Rainflow(extremalsS, extremalsT)
M = 0
S_{ref} = stressLVE(ε = 0.01, $\dot{\varepsilon}$ = 0.00014, log(a) = 0)
for i in range(length(fatigueHistory[0])) **do**
N, S_a, S_m, T = fatigueHistory[...]
$S_{a,R=-1}$ = $\sqrt{S_a + S_m \cdot S_a}$
$S_{a,R=0.1}$ = $\sqrt{\frac{9}{20}} \cdot S_{a,R=-1}$
loga = $\frac{Ea}{2.303 \cdot 8.314} \cdot \left(\frac{1}{T_r} - \frac{1}{T} \right)$
S = stressLVE(ε = 0.01, $\dot{\varepsilon}$ = 0.00014, loga = loga)
ratio = $\frac{S}{S_{ref}}$
B = -$A_r \cdot$ log(ratio)+B_r
$N_f = 10^{A_r \cdot log\left(\frac{S_{a,R=0.1}}{0.45}\right)+B}$
M = M + $\frac{N}{N_f}$
end for

3.4 Validation of the Digital Twin

In order to verify that the predictions of the Digital Twin were in line with its underlying theory, a few test cases were examined. The test cases were intended to qualitatively and quantitatively verify that the underlying theory was implemented correctly.

3.4.1 Creep

First, a comparison of creep resulting from 1MPa constant load, and the compliance function C(t) was performed. For the 1MPa constant load, the creep should be equal to C(t) after a time of approximately ten times the ramp period has passed [36].

Secondly, a sinusoidal loading was examined. In this case the creep (after an initial period) should be slightly out of phase with the stress [19]. This will result in the peak of the creep happening later than the peak of the elastic strain response.

Finally, it was shown that the TTSP, in the way it was applied, was valid. This was done by comparing the creep development for two equal load histories at different temperatures. If TTSP as applied is valid, it should be possible to do a horizontal shift of either of the creep-curves, so that it overlays the other in logarithmic time scale(excluding the ramp period). The shift should be equal to the shift factor calculated by Equation 2.12.

3.4.2 Fatigue

To test the Rainflow counting algorihm, and how it compares to the ATSM standard it was derived from, the predictions of the algorithm was compared to another public implementation of the ASTM E1049-85 Rainflow cycle counting algorithm [37]. Both a basic σ=sin(t) type loading, and a more complex σ=A·sin(B·t)+C·sin(D·t) were examined. Here t represents the time.

To test the ability of the algorithm to relate each cycle to its correct temperature, a stress-temperature history was chosen where σ=sin(t), T = t. Here T is the temperature. This means that the recorded temperature of each (half) cycle should be equal to the time of the cycle's last reversal.

3.5 Case study

In order to showcase the capabilities of the Digital Twin, it was decided to perform a case study. The case study considered a uniaxially loaded component, and its principles can be extended to any component loaded in a similar manner, such as a riser or the 0° layer in a 0/90° fiber orientation composite pipeline. In the case study the component was exposed to hypothesized loads and conditions, but it is the goal that it in the future the Digital Twin will obtain the loads and conditions from sensor data.

The goal of the case study was to compare the effect of different loads, temperatures on creep and fatigue development, including the effects of fluctuating loads/temperatures due to accidents, shut-downs, maintenance intervals, storms and so on. The case study was

also to compare the Digital Twin's predicted component lifetime compared to traditional constant maximum temperature, maximum load lifetime predictions.

When determining the lifetime of the component, failure was defined as follows:

1. Total strain reaching the elongation at break for a reference test (3,71%) [17] divided by a safety factor of 2,5. The reference test was performed on dry epoxy at 299K.

   Note that this is a novel way of defining failure by creep, which means that there is no industry established standards for the safety factor. Normally, failure due to sustained loads is defined by a empirical time criteria. In the DNVGL-ST-C501 standard, time to failure under static loads is calculated by the stress rupture formula on the form log(σ) = log($\sigma_{0,stressrupture}$) - β log(t), where $\sigma_{0,stressrupture}$ and β are experimentally determined constants. An approach similar to Miner's rule is used if there are several stress levels.

2. The Miner sum reaching 1 divided by a safety factor of 50. This safety factor is used in the DNVGL-ST-C501 and DNVGL-ST-F119 standards for safety class high composite components, and is designed to account for the uncertainty of the Miner sum in composites.

The load histories, as well as the values of the investigated parameters in the case study are hypothetical. Although they were chosen to be relevant for in-field use, they do not represent the actual real-life conditions in the field.

Note also that the qualitative effects of parameters such as temperature, stress level and moisture on creep and fatigue are already well known. What is brought to the table by the Digital Twin is the ability to perform a quantitative analysis of these effects. The advantage of the Digital Twin approach is the ability quickly and easily to analyze measured data, as well as making predictions based on assumed future data.

In the case study, three basic scenarios were considered:

- Fatigue dominated loading: Loading with large fluctuations, but mean load close to zero
- Creep dominated loading: Loading with little or no fluctuations, but non-zero mean
- Mixed loading: Loading with both large fluctuations and non-zero mean, inducing both fatigue and creep damage
- Temperature fluctuations

In addition, it was shown how temperature fluctuations and moisture affects the development of creep and fatigue damage.

After examining the basic cases, special cases were be considered, such as:

- Maintenance intervals that create periods with higher and lower loads
- Cases where the load levels decrease gradually during the lifetime of the component

- Accidents or other unexpected events that create abnormal loads, such as a storm or operating mistake of the well

Finally, the Digital Twin was used to compare Traditional lifespan calculation and investigate how much the component's lifetime can be extended beyond the original design life, by analyzing the components history of use when it is near the end of its original design life. Life extension will often be possible, due to how components are over-engineered to withstand loads that are greater than what is normally encountered. This is done because it is not possible to do a perfect forecast of the loads and temperatures a component will be exposed to.

After having calculated the effect of the history of use on the component and finding that both the creep strain and Miner sum are below the failure criteria, life extension can be calculated by assuming data for the future use of the component and redoing the analysis on the sum of measured and assumed data. The extent of life extension will therefore depend greatly on the type of assumed future data. There are two approaches for calculating the extent of the life extension:

- To calculate the remaining life where structural integrity of the component can be guaranteed, giving a lower bound for the remaining life, maximum load and temperature are assumed in the future. When this lower bound has been reached the procedure is repeated, incorporating the new sensor data that was obtained since the original end of life. With each repetition, the remaining life approaches closer to zero. The procedure can be repeated until the remaining life is deemed unacceptably short.

- A less conservative approach is to analyze the history of use and assume that the loading and temperature will be similar in the future to what has already been observed. This may give a more realistic estimate of the remaining life of the component but the method is non-conservative in the case of unexpected loads or temperatures arising.

  This approach can be made more conservative by assuming maximum load on the last day to which life extension is desired. The DNVGL-ST-C501 standard states that a component shall be able to endure its maximum intended load on its last day of service. This means that failure is considered when the residual strength is equal to the maximum load. Here, residual strength is defined as the load that causes the strain to raise above the failure criteria [3], or that a single cycle of that amplitude will cause the Miner sum to rise above 1.

Which approach that is more reasonable depends on the application. For designing and evaluating the integrity of the component, the first approach should be used. For getting a preliminary estimate of the cost of component replacement for the remainder of a project's lifetime, the second option may be better suited.

For the life extension case study, the examined conservative history of use was intended to give failure after about 25 years. It will then be examined if the lifetime of the component

[3]The stress required to raise the strain above the failure criteria will be lower if the component is already already strained due to creep

could be extended to 50 years or more by evaluating the actual history of use.

Figure 3.4 shows a schematic example of how the loads are assumed for the future in each of the aforementioned approaches, when after 50 months of use we are examining whether a life extension to 100 months is feasible or not.

Figure 3.4 Schematic illustration of the three ways to assume future loads when considering life extension

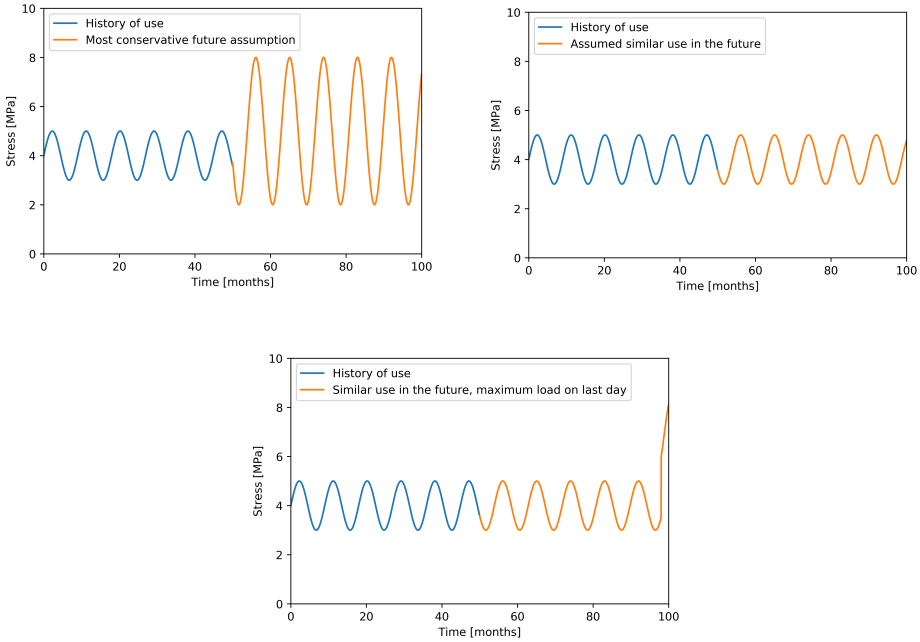

Chapter 4

Results

A short note on the presentation of the results:

The stress histories (in MPa) for each load history are given by the formula used to generate them in Python, where t is the time in seconds.

In some cases, the stress as given by the formula at t=0s is not zero. In these cases a linear ramp period, where the stress was increased from 0 to the stress at t=0s in the formula, was added to the loading history.

For the Rainflow counting, a gate of 0.1MPa was used and the binning/rounding was performed to the same level of precision.

4.1 Validation

4.1.1 Creep

Figure 4.1 shows a comparison of the Digital Twin's prediction of creep development from a constant 1MPa load, and C(t). For the 1MPa load, the ramp period was 5 seconds. The two curves were be equal after the ramp period. This result agrees agrees with the prediction in Section 3.4.

Figure 4.2 compares the elastic strain response and the creep resulting from a sinusoidal stress, and shows a vertical line where the peaks of each curve is located. The creep peaks happened slightly after the stress peaks. This result agrees agrees with the prediction in Section 3.4.

Figure 4.3 compares the calculated creep strain from a 1 MPa constant stress level for two different temperatures. The dashed line shows creep curve at 305K, after being shifted leftwards by a factor calculated from Equation 2.12. The shift factor resulted in the 305K

an 299K curves being equal after the ramp period. This result agrees agrees with the prediction in Section 3.4.

Figure 4.1 Comparison of creep from σ=1MPa, divided by 1MPa, and C(t). Ramp time 5s.

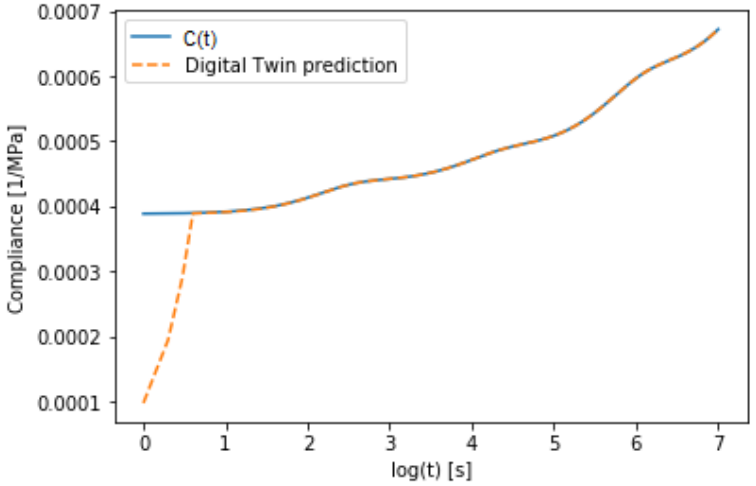

Figure 4.2 Comparison of creep and elastic strain response from a sinusoidal stress, σ=sin(0.25t), T=310K

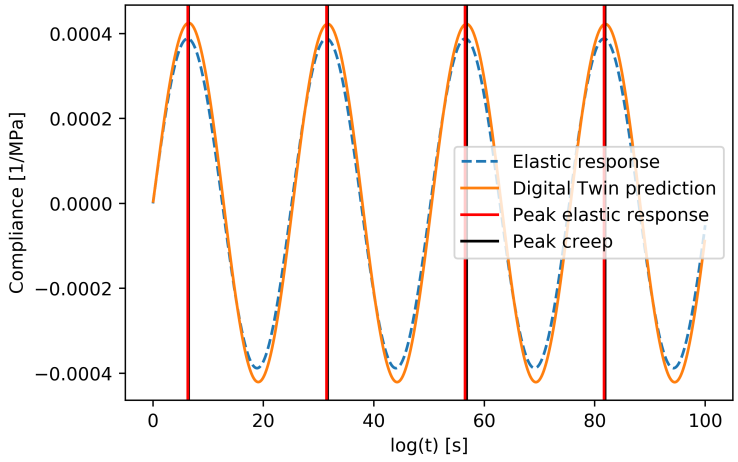

Figure 4.3 Comparison of the Digital Twin's predictions for different temperatures. σ=1 in both cases, log(a) = 0.951822

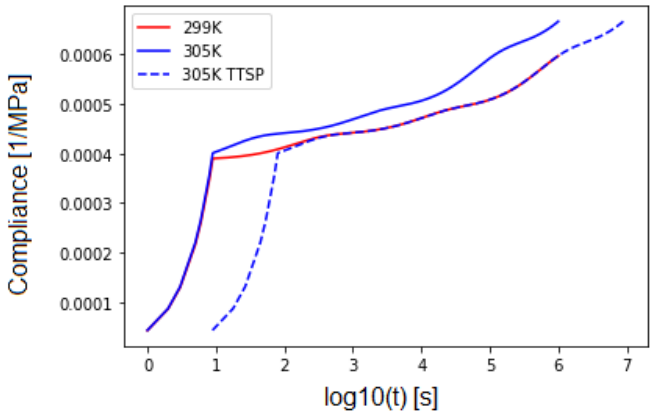

4.1.2 Fatigue

Decrease in static strength and cycles to failure from moisture saturation

Experimental results showed that the liquid saturation of the epoxy decreased the UTS by 19,8% at 296K, and that approximately the same reduction was observed for S_a at a given N_f [17]. Using LVE, calculating $\sigma(\varepsilon = 1\%)$, to approximate this decrease at the same temperature gave a reduction of 21.1%.

Figure 4.4 compares the experimental and predicted S-N curves for the liquid saturated epoxy. The agreement is best at low N. Since the X-axis is logarithmic, the errors at N$> 10^5$ are quite significant. At S_a = 7MPa, log(S_{max}) = 1.2, the percentage difference between N_f as predicted by experimental results and the Digital Twin is 54%.

Figure 4.4 Comparison of S-N curves of saturated epoxy, for R=0.1. On the Y-axis, S_{max} means the maximum stress during a cycle. For this R-ratio, $S_{max} = \frac{S_a}{0.45}$

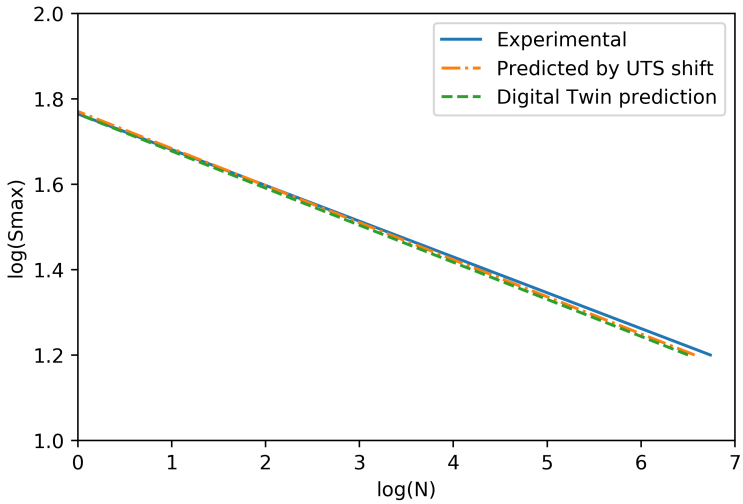

Rainflow counting

Figure 4.5 shows a basic sinusoidal loading. For this stress history, the Digital Twin's and alternative implementation of ASTM E1049-85's counted cycles are listed in Table 4.1. Each column gives the relevant information (S_a, S_m, N) for each type of cycle. The two implementations of the Rainflow counting gave equal results.

Figure 4.6 shows a more complex sinusoidal loading. For this stress history, the Digital Twin's and alternative implementation of ASTM E1049-85's counted cycles are listed in Table 4.2. The two implementations of the Rainflow counting gave equal results.

Figure 4.7 shows a basic sinusoidal loading where the temperature increases linearly with time. For this stress history, the Digital Twin's counted cycles are listed in Table 4.3. Each

cycle was attributed its correct temperature.

	Digital Twin	ASTM E1049-85
S_a	1	1
S_m	1	1
N	3,5	3,5

Table 4.1: Cycles counted by Digital Twin and ASTM E1049-85 for the stress history in Figure 4.5

Figure 4.5 Stress history, σ=sin(0.5t), counted in Table 4.1

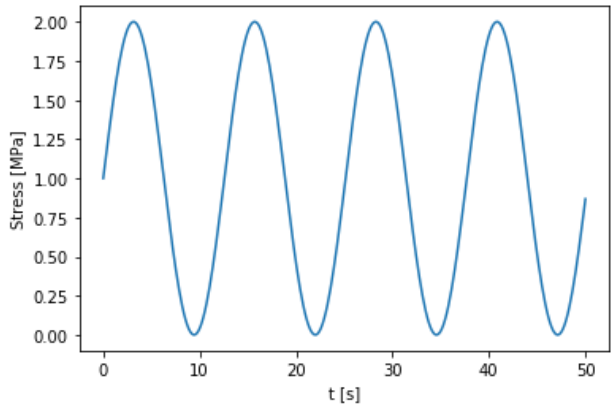

	Digital Twin		ASTM E1049-85	
S_a	1,3	2,7	1,3	2,7
S_m	0	0	0	0
N	4	3,5	4	3,5

Table 4.2: Cycles counted by Digital Twin and ASTM E1049-85 for the stress history in Figure 4.6

	Digital Twin			
S_a	1	1	1	1
S_m	0	0	0	0
N	0,5	0,5	0,5	0,5
T	15	25	35	45

Table 4.3: Cycles counted by Digital Twin for the stress history in Figure 4.7

Figure 4.6 Stress history, σ = sin(0.5t)+2sin(t), counted in Table 4.2

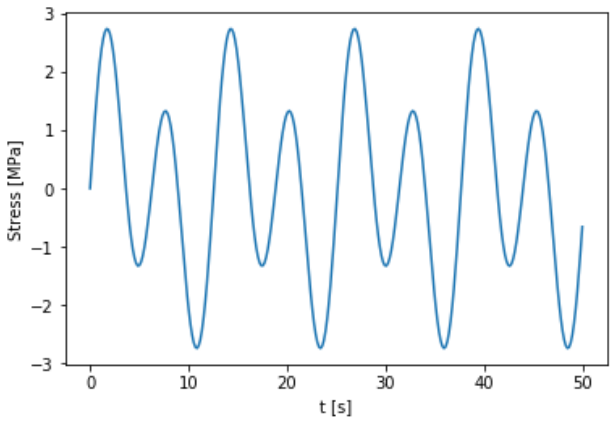

Figure 4.7 Stress history with linearly increasing temperature, σ = sin(0.1π·t), T=t. Counted in Table 4.3

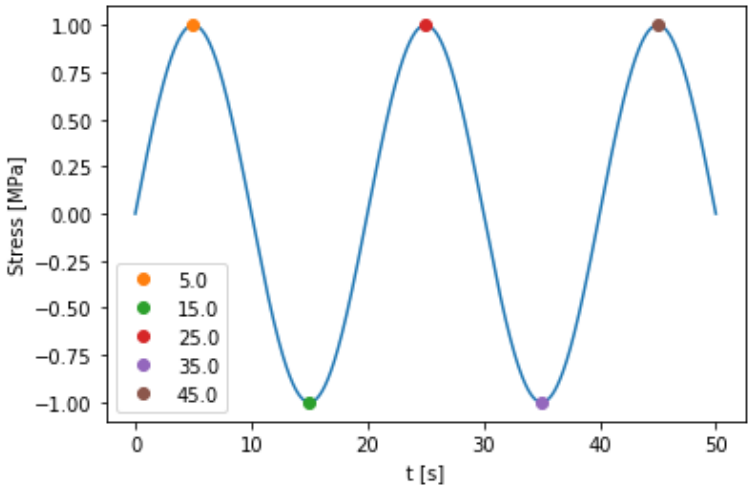

4.2 Case study

Note that unless otherwise is stated, the calculations are done for dry epoxy at 299K. A ramp time 10s was used where necessary.

In the following figures the red line represents the creep, the blue line represents the Miner's sum, and the black dashed line represents the elastic part of the strain. This line will be proportional to the stress level experienced by the component, and is included to give an idea of the loading/stress history.

4.2.1 Basic cases

To demonstrate the capabilities of the Digital Twin, the fatigue and creep behavior of the component is shown for the three basic loading cases: constant load, fluctuating load with zero mean, fluctuating load with non-zero mean. It will also be shown how moisture and a temporary temperature increase affects the development of creep and fatigue.

Figure 4.8 Creep and fatigue damage for a load without fluctuations. $\sigma = 1$

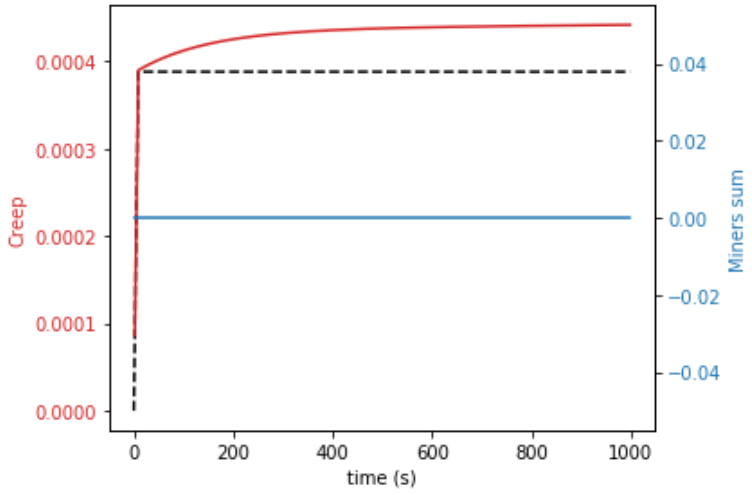

Figure 4.9 Creep and fatigue damage for a fluctuating stress with zero mean. $\sigma = \sin(0.5t)$

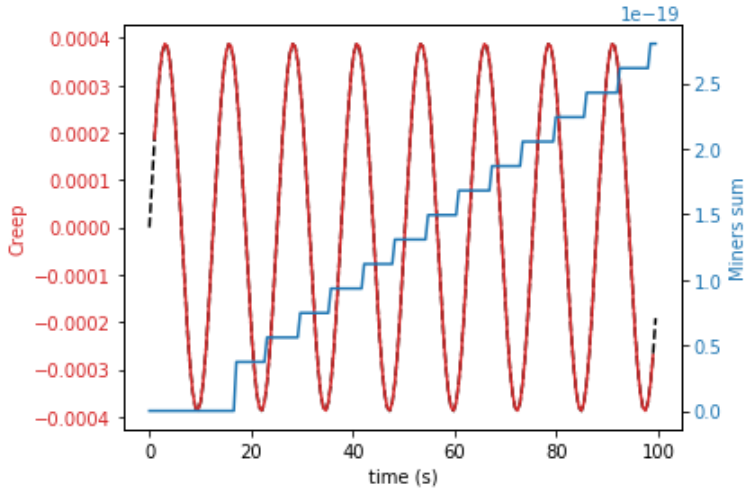

Figure 4.10 Creep and fatigue damage for a fluctuating stress and non-zero mean. $\sigma = \sin(0.5t)+5$

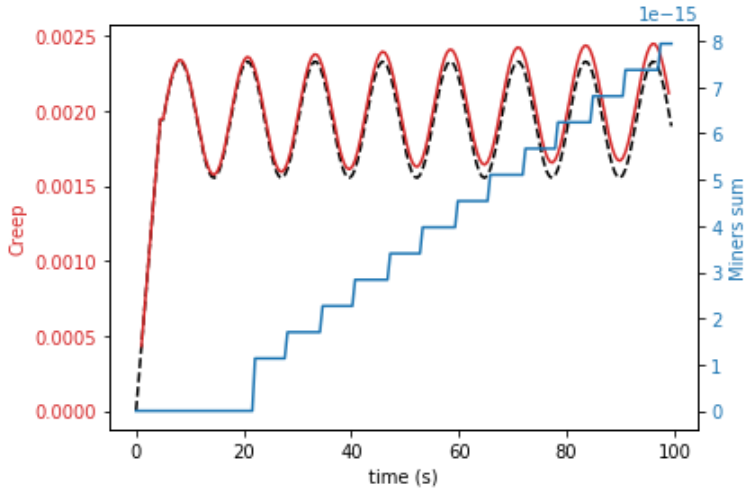

Figure 4.11 Creep and fatigue damage development, showing the influence of temperature. σ = sin(0.4t)+15. For t$\in$ [500s, 600s], T = 309K

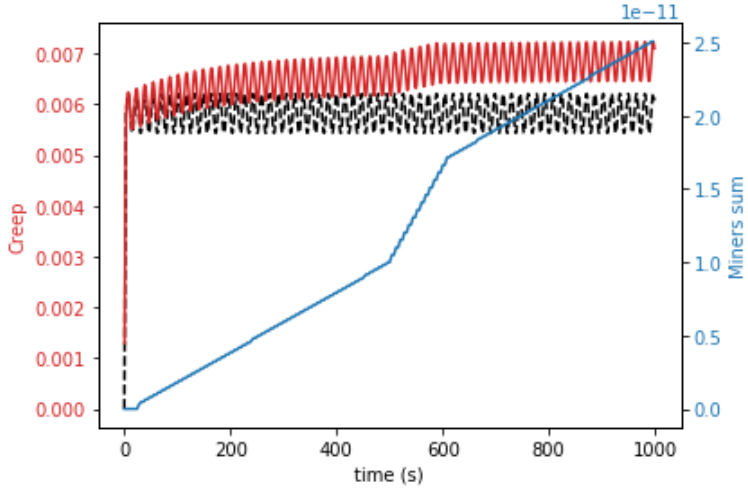

Figure 4.12 Comparison of creep/fatigue in dry and saturated epoxy. S = sin(0.4t)+15

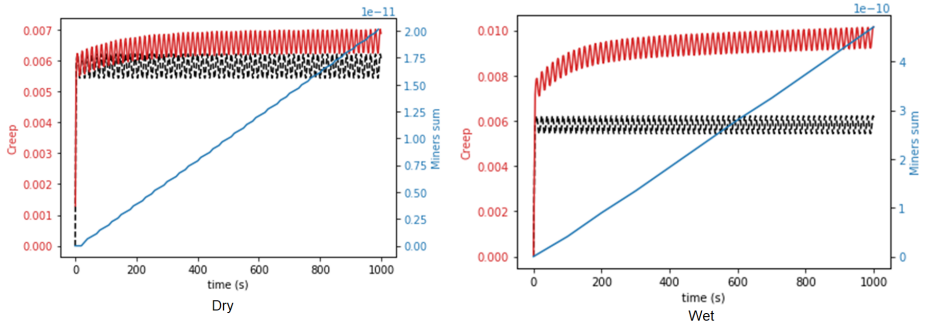

4.2.2 Special cases

In the following Section are shown creep and fatigue calculations for the special cases.

Maintenance intervals

For the maintenance intervals case, the stress was given by Equation 4.1. The development of creep and fatigue damage is shown in Figure 4.13.

$$\sigma = \begin{cases} sin(0.5t) + 10 & t \in [200s, 300s], [500s, 600s] \\ 0.5 \cdot sin(0.5t) + 5 & t \notin [200s, 300s], [500s, 600s] \end{cases} \tag{4.1}$$

For the normal operation, the Miner sum increased much faster than during the maintenance period where the Miner had almost no increase. Interestingly, the Miner sum rose abruptly at the beginning and end of each maintenance period.

Creep strain increased during the normal operation, but decreased in the maintenance intervals even tough the mean stress was above zero.

Accident

For the accident case, the stress was given by Equation 4.2. The development of creep and fatigue damage is shown in Figure 4.14.

$$\sigma = \begin{cases} 3 \cdot sin(0.2t) + 5 & t \notin [500s, 700s] \\ 4 \cdot sin(0.4t) + 10 & t \in [500s, 700s] \end{cases} \tag{4.2}$$

For the normal operation, the Miner sum increased very little compared to during the accident. Also for this case, the Miner sum rose abruptly at the beginning and end of the accident period.

The creep strain increased steadily before the accident, and at a higher rate during the accident. After the accident, the strain decreased despite a greater than zero mean stress.

Gradually decreasing load

Two types of gradually decreasing loads were examined. The first type is given by Equation 4.3. For this type, the development of creep and fatigue damage is shown in Figure 4.15.

$$\sigma = \frac{-3}{1 + e^{-0.01(t-1000)}} (5 \cdot sin(t) + 4) \tag{4.3}$$

From Figure 4.15 it is evident that this load caused the creep first to increase when the stress was stable, and then decrease when the stress decreased. The creep stabilized above the elastic response. The Miner sum initially increased almost linearly, before slowing down, then increasing, and finally leveling off as the stress stabilized.

The second type is given by Equation 4.4. For this type, the development of creep and fatigue damage is shown in Figure 4.16.

$$\sigma = e^{-0.001t}(5 \cdot sin(0.2t) + 25) \tag{4.4}$$

From Figure 4.16 it is apparent that for this load the creep strain was decreasing continually, but stabilized slightly above zero. The Miner sum first accelerated, before slowing its increase and leveling off.

Figure 4.13 Creep and fatigue damage development for maintenance intervals, where the stress mean and fluctuations is lower in periods

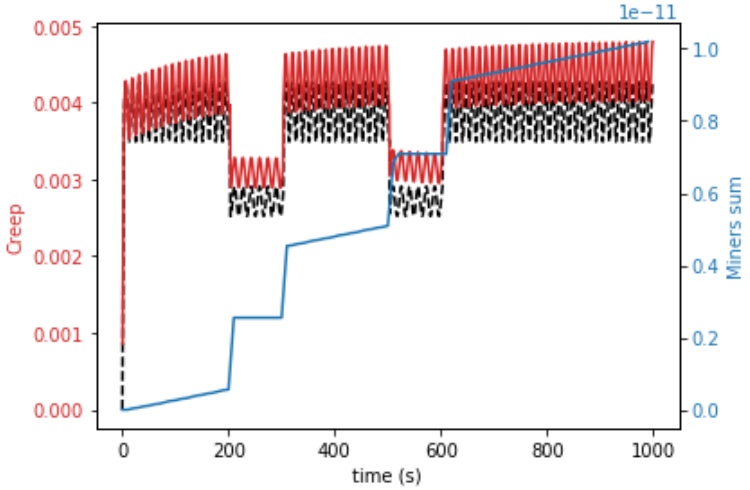

Figure 4.14 Creep and fatigue damage development for an operating accident or storm causing abnormal loading

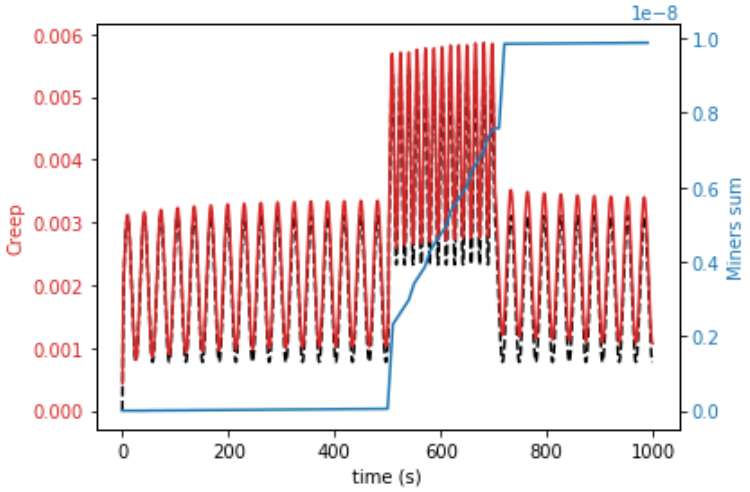

Figure 4.15 Creep and fatigue damage development for a gradually decreasing load, first type

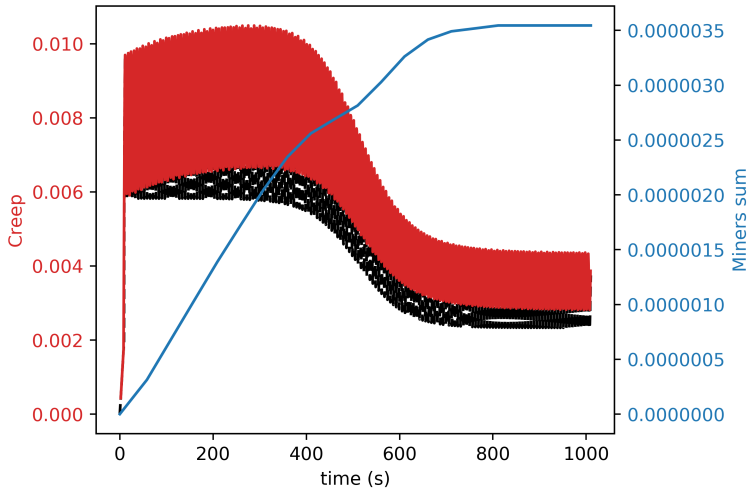

Figure 4.16 Creep and fatigue damage development for a gradually decreasing load, second type

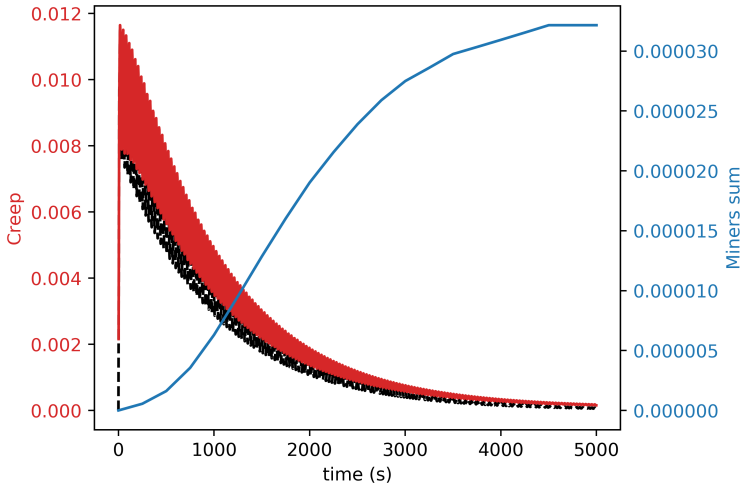

4.3 Life extension

In this section, in order to reduce computational time, the creep was only plotted every 22,36 weeks (13524142s). This plotting frequency plots tops and bottoms in the stress history alternatively. The temperature for all of the three cases was 288K.

4.3.1 Conservative history of use

Figure 4.17 shows the conservative, severe history of use considered in the design phase during the construction of the component. This stress history is given by Equation 4.5, where t is the time in seconds. This level of loading resulted in failure by fatigue after approximately 25 years, but failure due to creep was not expected.

$$\sigma = 6 \cdot sin(0.0044578 \cdot t) + 15 \tag{4.5}$$

4.3.2 Conservative life extension

Figure 4.18 shows the the most conservative approach for life extension. For the initial 25 years, the actual history of use was considered, while for the remainder of the lifetime, the loads are conservatively assumed to be the same as those considered in the design phase. The actual history of use is given by Equation 4.6. This history of use resulted in failure by fatigue after about 40 years, but failure due to creep was not expected.

$$\sigma = \begin{cases} 6 \cdot sin(0.0044578 \cdot t) + 15 & Years : 0 \rightarrow 5, 10 \rightarrow 15 \\ 3 \cdot sin(0.0044578 \cdot t) + 12 & Years : 5 \rightarrow 10, 15 \rightarrow 25 \end{cases} \tag{4.6}$$

4.3.3 Life extension assuming similar future loads

Figure 4.19 shows what happens if the future loads are assumed to be the same as the initial 25 years, as shown in Equation 4.7. In this case, the component is predicted to remain in operation for over 50 years before failure is expected to occur. Note that assuming the maximum load to occur once after 50 years would not result in failure due to creep, since failure by creep did not happen in Figure 4.18, and the Miner sum is far enough from 0.02 that a single cycle would not result in failure.

$$\sigma = \begin{cases} 6 \cdot sin(0.0044578 \cdot t) + 15 & Years : 0 \rightarrow 5, 10 \rightarrow 15, 25 \rightarrow 30, 35 \rightarrow 40 \\ 3 \cdot sin(0.0044578 \cdot t) + 12 & Years : 5 \rightarrow 10, 15 \rightarrow 25, 30 \rightarrow 35, 40 \rightarrow 50 \end{cases} \tag{4.7}$$

Figure 4.17 Creep and fatigue damage development for the conservative history of use

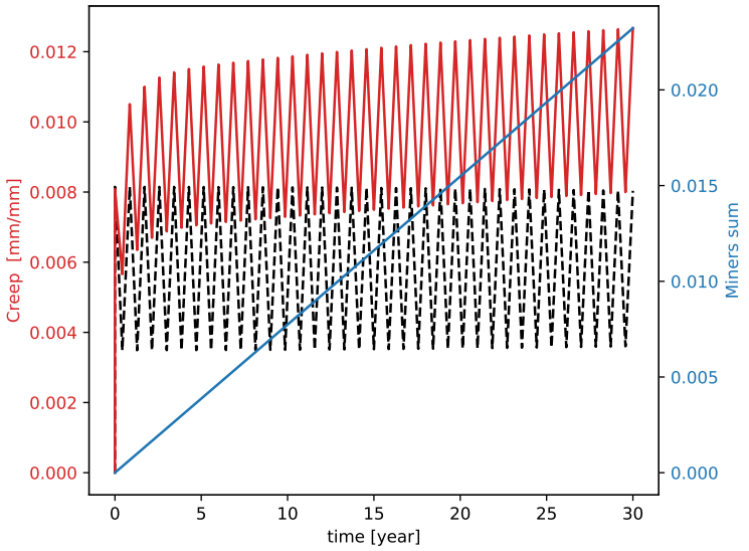

Figure 4.18 Conservative life extension by considering actual history of use, and appending a conservative assumption for the future

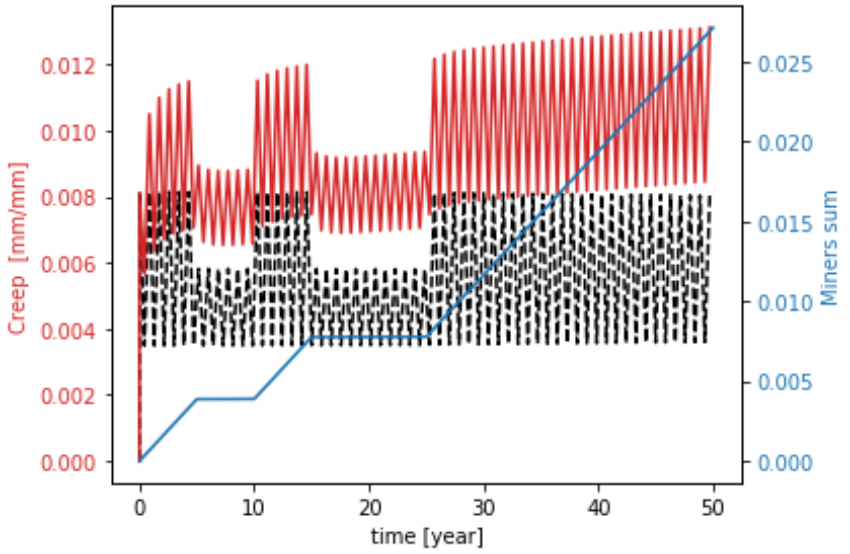

Figure 4.19 Life extension considering actual history of use, and assuming that loads will be similar in the future

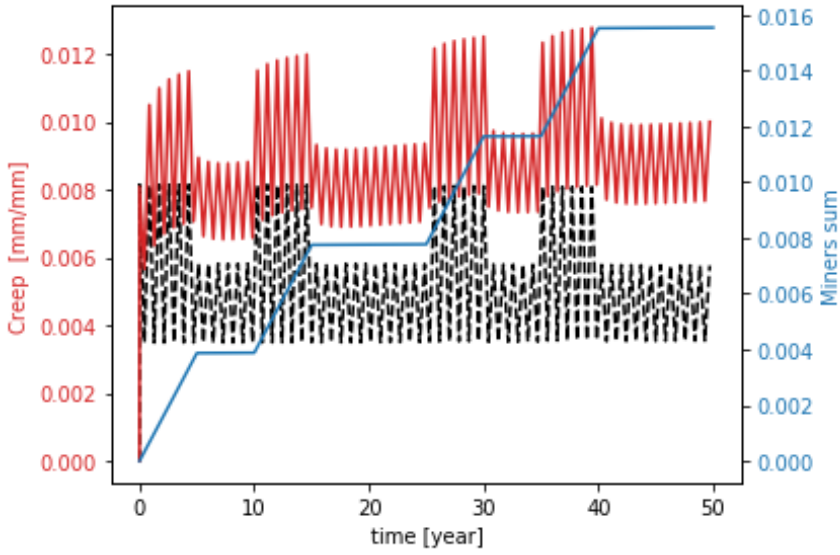

Chapter 5

Discussion

5.1 Validation

As evident from the figures in Section 4.1, the predictions of the Digital Twin were qualitatively and quantitatively correct for the basic cases within the creep domain. For fatigue, it was also evident that the modified version of the Rainflow counting algorithm counted correctly.

The estimated reduction in UTS by reduction at ε=1% was off by 1.1 percentage points, compared to experimental results of UTS reduction [17]. This can be considered acceptable, but it has not been demonstrated that the Digital Twin is able to estimate static strength changes due to temperature fluctuations.

With respect to the S-N curve, it was apparent that the Digital Twin was able to predict the curve of the saturated epoxy reasonably well. Due to the relatively flat shape of the S-N curve, the error in S_a at a given N_f is relatively small, but the error in N_f at a given S_a (which is used by the Digital Twin to calculate the Miner sum) was much higher. The largest deviations from the experimental S-N curve were observed for large N [1], which is significant since the scale is logarithmic. For large N the fatigue strength was underestimated, which is a error in the conservative direction. For better quantitative agreement, shifting the S-N curve based on UTS measurements may be the preferred option, although neither of these methods are perfect.

A factor that is not considered by the Digital Twin is the increased ductility for conditioned material/higher temperatures, which may lead to higher elongation at break. This means that the Digital Twin may predict failure by creep to happen too early for saturated epoxy or at higher temperatures, but this is an error in the conservative direction.

[1] Extrapolation error is likely responsible for parts of the deviation between the experimental and predicted S-N curve. In the original source of the S-N curves, S-N testing was only performed for $N < 10^6$

5.2 Case study

5.2.1 Basic cases

From Figures 4.8, 4.9, 4.10 it is apparent that the Digital Twin calculated the development of creep and fatigue as expected:

- When there was a mean stress but no stress fluctuation, only the creep increased as a function of time.
- When the mean stress was zero, but the stress is fluctuated periodically, the acquired strain was dominated by the elastic/instantaneous part of the creep while the Miner sum increased linearly.
- When there was both periodic fluctuations and a non-zero mean stress, both strain and Miner's sum increased as functions of time.

In Figures 4.9, 4.10 the Miner sum increased in a step-wise fashion, where each step coincides with a reversal in the stress history and the first step happening after three reversals. This is consistent with the aforementioned ATSM Rainflow counting standard, where only finished cycles are counted and three reversals being the minimum to constitute a full cycle.

Increased temperature or liquid saturation accelerated the creep-rate and slope of the Miner's sum. What is interesting to note is what happened when the temperature was increased, and then returned to its previous level. The Miner's sum returns to the same slope as before the temperature was increased. The creep-rate on the other hand, will increase at a lower rate after the temperature is reversed, than what it would have done at the same time if the temperature had remained constant. Note that although the creep rate was lower after the period of increased temperature, the total creep was higher than what it would have been if the temperature was never increased.

This can be explained by the creep-rate decreasing over time when the temperature is constant. When the temperature is increased it effectively accelerates the passage of time, which means that a later point on the constant-temperature creep curve is reached faster. This is illustrated in Figure 5.1, which shows a generic creep curve for constant temperature. Consider a case where the temperature is elevated in the time span t1-t2, so that time is accelerated by a factor of three. Now the creep between t1 and t3 will happen within the time span t1-t2. The result is shown in Figure 5.2, where creep is plotted with the time span t1-t3 compressed into t1-t2. When the temperature is decreased to its initial level, creep continues with the slope at t3 in Figure 5.1. If temperature was not changed, creep continues with the slope at t2.

5.2.2 Special cases

Maintenance intervals

Both the creep and Miner's sum increased faster during the periods of higher load amplitude/mean.

Figure 5.1 Generic constant load/temperature creep curve

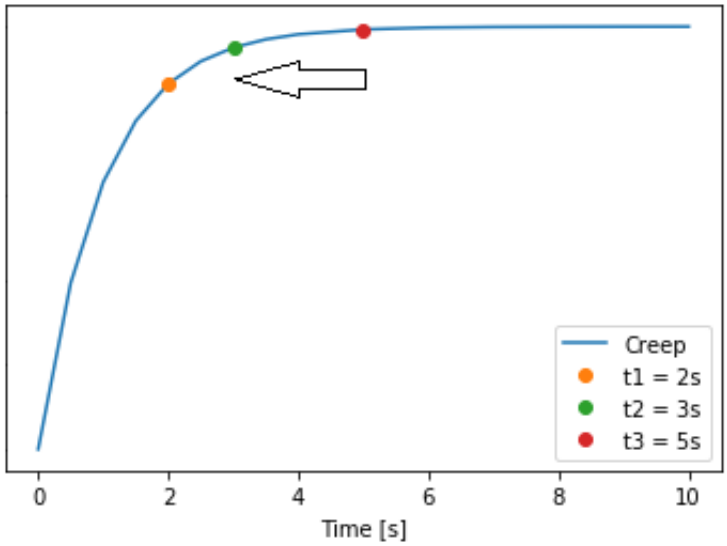

Figure 5.2 Generic constant load creep curve, after the temperature effect was included. Temperature increase between 2s and 3s. log(a) = log(3). At t=3s, the slope of the constant T curve is higher than that of the non constant T curve

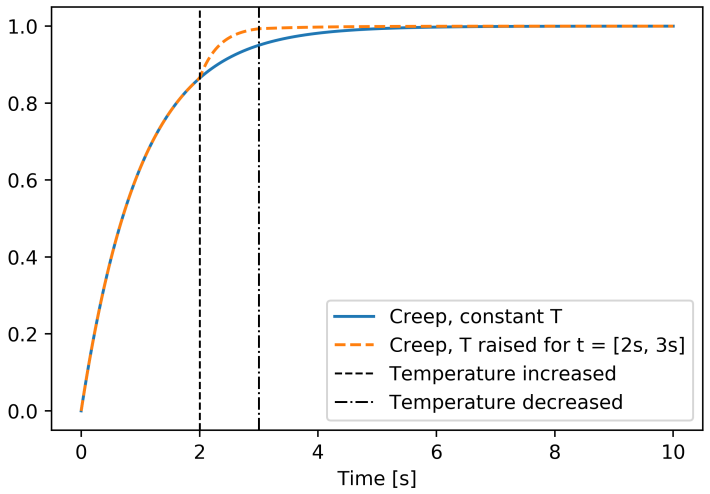

What is interesting to note is that the abrupt increase in Miner sum in the transition between high load/amplitude to lower load/amplitude. This abrupt increase is caused by the large amplitude cycle created in this transition, since the change in mean stress is large. If there

is many of these transitions, they may end up having a significant effect on the Miner's sum, meaning that fatigue damage accumulates faster when there are periods of lower load mean/amplitude. Note that the result obtained is for an extreme case, where the difference in mean stress is large compared to the stress amplitude.

While the Miner's sum continued to rise during the smaller load amplitude/mean period, the strain on the other hand decreased for the first period after a high amplitude/mean load period. This phenomenon is called recovery and is in line with the predictions of LVE theory. If the low amplitude/mean load period were maintained for an extended period, the creep would start increasing again, as is seen in Figure 4.18. Note that this is a type of history where the maximum strain during the component's lifetime does not necessarily happen at the longest times. In this case it might therefore be necessary to also find the maximum creep during the component's history of use, rather than the creep after a given history of use.

Accident

The effect of an operating mistake/accident was (qualitatively) quite similar to the effect of maintenance intervals that causes periods of higher and lower stress. The low amplitude/mean to high amplitude/mean transition also here created its own cycle, which ended up affecting the Miner sum. For the first period after the accident, we also saw a certain recovery in the creep strain.

Gradually decreasing mean/amplitude

The trend in both Figure 4.15 and 4.16 is that the total creep strain decreases when the stress is reduced. This is due to a decrease in the elastic part of the strain. It is worth to note that the creep will stabilize above the elastic strain, due to the viscous creep that happened during the high stress period.

The development of fatigue exhibited a somewhat counter-intuitive behavior for this type of loading. Intuitively for this type of loading, one would expect the Miner's sum to have a shape similar to that of the logarithmic function (strictly decreasing slope, negative second derivative), since both S_a and S_m are decreasing. In Figures 4.15 and 4.16 on the other hand, the Miner sum is growing the fastest during the period where S_m is decreasing the quickest. What causes this rather strange phenomena is the way the Rainflow counting evaluates the decreasing S_m. The half-cycle from maximum stress of the earliest cycle down to the minimum stress of the latest cycle, grows as S_m is decreasing. This cycle has high amplitude compared to the other cycles. These can be treated as interruptions of this larger half cycle. The large half cycle ends up having a significant effect on the Miner's sum. Figure 5.3 illustrates how the early-maximum-to-late-minimum half cycle grows as S_m decreases. As time passes, the growth of this half cycle slows down, making the Miner sum level off.

Note that the results obtained in this instance are exaggerated. If S_m was decreasing slower, along with a higher load frequency and amplitude, the slope of the Miner's sum would behave more in line with expectations.

Figure 5.3 Growth of maximum-minimum half cycle and development of Miner sum for gradually decreasing load. Maximum-minimum half cycle marked in red. Stress history in black.

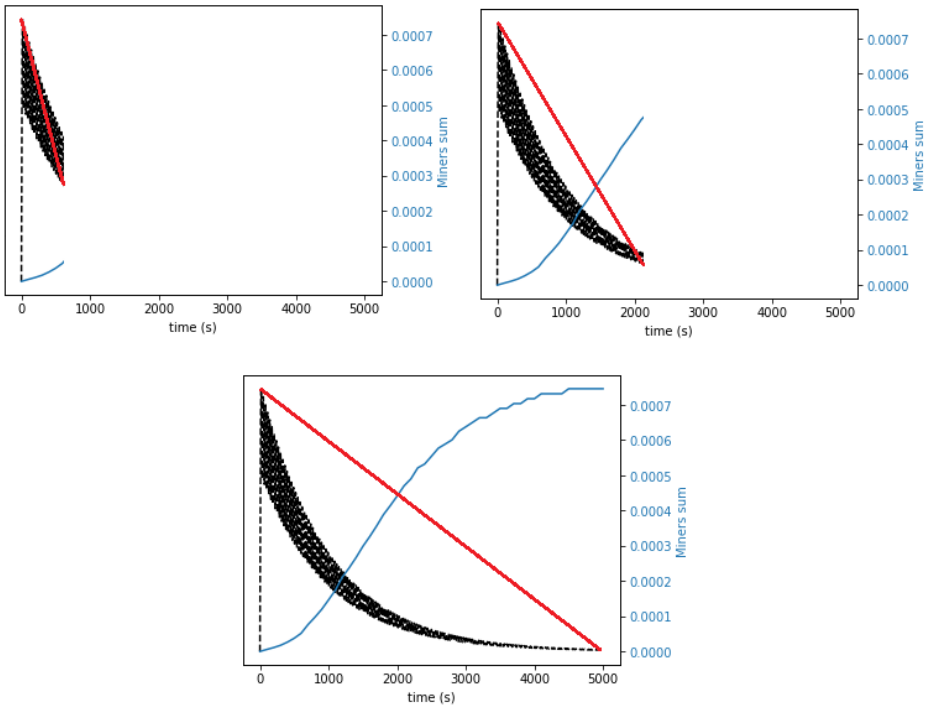

Life extension

When a more realistic and less severe history of use was considered, both Miner's sum and creep developed slower. This resulted in predicted failure occurring later. For the given history, it was possible to extend the life of the significantly using the most conservative life extension technique. When the less conservative technique was used, the estimated life of the component was more than doubled.

How much it is possible to extend the life of the component using this technique depends greatly on the difference between the severe conditions of the design phase and the actual measured conditions.

In addition to considering the effect of less severe histories, the Digital Twin can also be be used to examine the effects of more severe histories. If a component is briefly exposed to loads or temperatures it is not qualified for, the Digital Twin can be used to check whether or not the component needs to be replaced. Even if a component is incidentally exposed to loads or temperatures above its qualification range, the total creep and fatigue accumulated during the component's lifetime may still be below the failure criteria.

5.3 Coding

During the development of the Digital Twin, the focus was placed on creating a viable concept that had a clear link to the underlying physical models.

The Digital Twin was coded in Python. Python is among the most popular programming languages for scientific use. Python has support for cross-linking with important software for performing FE-calculations, such as *Abaqus*. Python is also popular for machine learning. The main drawback of Python is that its computational performance (speed of performing calculations) is worse than lower level languages such as C++.

The code of the Digital Twin was not optimized with respect to computational efficiency/running time. This means that the running time of the program can be quite long if a long history of use with high sensor sampling frequency is to be analysed. Especially the *find_peaks* algorithm used for Rainflow counting can use very long time for long loading histories.

There are several possibilities for optimization of the running time of the code. Maybe the biggest improvement may be gained from implementing *multiprocessing*. Multiprocessing means that several calculations are run in parallel, which uses more processing power but can reduce computational time significantly. Multiprocessing can easily be implemented for calculating the variable creepStep in Algorithm 2, as well as for the for-loop running through the fatigue history matrix in Algorithm 5, calculating N/N_f for each type cycle. It is also possible to optimize this fatigue history matrix, which currently contains individual cycles. If all cycles where S_a, S_m, T, and C_{H_2O} are equal were combined, summing N, calculating the Miner sum would be quicker. Multiprocessing could also potentially be implemented to *find_peaks* algorithm, by splitting the stress history into several lists, and finding the peaks in each list in parallel.

5.4 Reliability of results

Qualitatively, the Digital Twin's predictions were as expected for all cases, except when the mean stress and amplitude were decreasing rapidly. Even though the latter was a somewhat counter-intuitive result, it is in line with the underlying theory of the Twin. There are several factors to be discussed when evaluating the reliability of the Digital Twin's predictions.

The old saying *garbage in equals garbage out* is a good illustrator for the Digital Twin. The Digital Twin is only as good as the underlying degradation models. If these are implemented correctly, errors in predictions can only be caused by the degradation models being fundamentally flawed. Judging from Section 4.1, there is nothing to suggest that the degradation models have been implemented incorrectly. Nevertheless, the counter-intuitive result for the rapidly decreasing mean stress may indicate that the combination of Rainflow counting, SWT mean stress correction, and Miner sum has its limits, and is not a perfect way to calculate fatigue life for complex loading histories in polymers.

Rainflow counting is the most popular way to evaluate fatigue loading where the mean and amplitude is fluctuating. Despite this, application of the rule on loading histories such as

the ones in Figure 4.15, 4.16 resulted in somewhat counterintuitive results. It is well known that Rainflow counting is best suited for loading histories that are random or periodical in nature. This means that the user of the Digital Twin must be cautious when analyzing load histories like the ones illustrated in Figures 4.15, 4.16.

LVE was used to predict creep, as well as estimating changes in ultimate tensile strength due to temperature and moisture, which in turn was used to estimate the fatigue strength as a function of these environmental parameters. The validity LVE depends on several factors such as stress level, temperature, loading rate and moisture. Typically, LVE is assumed valid up to ε=1%. In this work, LVE was used for creep strains up to 1,5%. This may introduce an error in the results.

Another source of error is the way changes in static strength for the epoxy is calculated. Although the decrease due to liquid saturation at 296K was modelled with little error, it has not been demonstrated that it works for other temperatures. Uni-axial fatigue strength as a function of pure temperature changes has not been tested and is therefore not demonstrated to follow the same pattern as for moisture uptake.

5.5 Benefits and drawbacks of the Digital Twin approach

5.5.1 Benefits

As mentioned, the strength of the Digital Twin is to quantitatively analyze the effect of different parameters that affect creep and fatigue development in polymers. The most common currently existing methodologies have only considered these effects individually.

As mentioned in Section 1.2, a less intensive testing regiment is one of the possible benefits of utilizing physical degradation models in a Digital Twin. LVE theory was used to calculate material properties for different use and environmental parameters. These would normally have to be determined experimentally. Since this use of viscoelastic theory is not yet well established, the benefits of less testing will initially not be that significant since one still will need to do confirmatory tests. Once more confidence is earned, the extent of testing can be reduced.

Maybe the greatest benefit of the Digital Twin is the possibility to extend component lifetime. In addition to the procurement cost of the component, savings are also incurred by limiting on-site inspections, as well as avoiding shutdowns and production stops. Being able to monitor the condition of a component in real time gives both cost and safety benefits.

5.5.2 Drawbacks

In addition to the benefits, there are also some drawbacks or costs associated with the Digital Twin. The most obvious costs are related to the instrumentation of the components, plus the cost of transmitting or retrieving the sensor data. Currently, instrumentation of components is rarely done because the cost is thought to outweigh the benefits since there is a lack of methodology to draw useful insights from the sensor data. It is the belief of

the author that to the contrary, that the Digital Twin approach, with the prospect of life extension, makes instrumentation of components worthwhile.

Another more abstract cost is the insecurity associated with the Digital Twin. Before confidence is earned, many operators may be hesitant to use a less conservative when evaluating component lifetime and integrity. Extensive testing and further refining and development will likely be needed before the Digital Twin approach can be used in practice.

As mentioned, the Digital Twin's predictions are only as good as its underlying theory. Since the Digital Twin approach is less conservative in nature, errors in the underlying theory will be more critical than with currently used methodologies. Since the Digital Twin combines and leverages several physical and empirical models, a error in one model may propagate into the others. One example of this is how the small error in predicted UTS reduction turned into a much larger error for predicted N_f in Section 4.1.2. The need to develop accurate models for the polymer's long term behavior when exposed to in-field conditions is therefore accentuated by the Digital Twin.

Note that one method to circumvent the uncertainty associated with the Digital Twin would be to test the material properties (cycles to failure, stress rupture time) for every combination of loading and environmental parameters that the component could reasonably be expected to be exposed to. The Digital Twin would then evaluate the component's history of use data based on actual test results and empirical data models, using Miner sum type of approach to predict failure for both creep and fatigue [2]. The immense testing regiment required would be the primary disadvantage of such an approach.

In Section 4.1, it was shown that the error in the Digital Twin's prediction was conservative (underestimation of fatigue life), but this will not necessarily always be the case. An error in the conservative direction is also unwanted, since it may lead to increased project costs (components are replaced before they need to), negating one of the primary goals of the Digital Twin.

[2] In the DNVGL-ST-C501 standard a similar approach to Miner sum, where t/t_f is summed for the different conditions. Here t is the time elapsed at a set of conditions, t_f is the stress rupture time at the same conditions

Chapter 6

Conclusion and further research

6.1 Conclusion

A Digital Twin for a uniaxially loaded polymer component was developed. The Digital Twin was made using a limited set of experimental data consisting of reference creep, tensile and fatigue tests. Linear viscoelastic theory was used to predict creep behaviour and fatigue strength as functions of environmental parameters. Rainflow counting was used to reduce a load history to a series of fatigue cycles, while Miner sum was used to evaluate the damage inflicted by these.

For the most basic load/temperature cases, where experimental data was available, the predictions of the Digital Twin within the creep domain were in line with experimental results. The calculated decrease in ultimate tensile strength for the saturated epoxy compared to dry also showed good agreement with experimental results, but the moisture's quantitative effect on fatigue life was not modelled to a satisfactory degree of accuracy. It may be better to model the temperature/moisture effect on fatigue life based on the experimentally determined shift in static strength.

For the more complicated cases, with more complicated load/temperature histories, the predictions of the Digital Twin could not be validated quantitatively due to a lack of experimental results, but from a qualitative point of view they were in line with the underlying theory.

A Digital Twin approach as described in this work can contribute to significant cost savings during the testing, design, and operation phases of a project. These savings are related to a less intensive testing regiment (test reference cases, and calculate the rest), ease of calculating material behavior, less conservatism needed when considering component lifetime and strength, as well as limiting the need for on-site inspections.

Although there is a cost and difficulty associated with measuring the loads and tempera-

tures/moisture level that are needed for the Digital Twin to perform its calculations, the potential benefits as demonstrated in this work are considerable. From the author's point of view it is probable that they will outweigh the costs.

6.2 Future research

Although the Digital Twin concept demonstrated in this work has shown great potential, it is still a long way to go before it can be in implemented in real-world projects. The author suggest the following research to be done:

- Perform creep and fatigue experiments for a range of loading, temperature and moisture conditions, as well as combinations of these, so that the predictions of the Digital Twin can be validated for more complex cases.
- Perform experiments to compare the traditional creep rupture time approach and the creep strain approach used in this work for predicting failure due to sustained loads. It will be interesting to see how the time to failure compares between the methods, since it is possible they will be quite similar.
- Create interface towards FEA software so that the Digital Twin can evaluate more complex loading modes, or so that the material parameters calculated by the Digital Twin may be used in a FEA analysis. It may also be needed to refine some of the equations for calculating viscoelastic mechanical response into their three dimensional forms [19].
- Create the instrumentation/sensors required for the component modelled by the Digital Twin and connect them to the IoT, so that a component's condition can be monitored remotely in real time.
- Implement the TTSP for a sample not fully saturated with liquid. To do this one must calculate diffusion within the polymer, as well as establish the material's properties such as glass transition temperature as functions of liquid concentration.
- Further refine and develop physical models for fatigue and creep in polymeric and composite materials. It will be especially important to find a model that models the link between creep and fatigue damage.

Bibliography

[1] Rod Martin. Composite materials: An enabling material for offshore piping systems. Houston, Texas, 2013. Offshore Technology Conference.

[2] Trifunovi Prvoslav. Use of composite materials in oil industry. *Underground Mining Engineering*, 19:157–164, 2011.

[3] Elizabete Lucas, Claudia Mansur, Luciana Spinelli, and Yure Queiros. Polymer science applied to petroleum production. *Pure Appl. Chem*, 81:473–494, 03 2009.

[4] A. Echtermeyer. Integrating durability in marine composite certification. *Solid Mechanics and its Applications*, 208:179–194, 11 2014.

[5] A. Gagani. *Environmental Effects on Fiber Reinforced Polymer Composites, PHD Thesis*. NTNU, Faculty of Engineering Department of Mechanical and Industrial Engineering, 2019.

[6] A. T. Echtermeyer A. Gagani, A. Krauklis and T. Mazan. Multiscale modelling of environmental degradation—first steps. In *Durability of Composites in a Marine Environment 2*, pages 135–149. Springer, 2018.

[7] D. Kuhlman. *A Python Book: Beginning Python, Advanced Python, and Python Exercises*. Open source MIT licence, 2013.

[8] A. D. McNaught and A. Wilkinson. *IUPAC. Compendium of Chemical Terminology, 2nd ed*. Blackwell Scientific Publications, Oxford, 1997.

[9] P. M. Lardizabal J Colmenero. Are polymers standard glass-forming systems? the role of intramolecular barriers on the glass-transition phenomena of glass-forming polymers. *Journal of Physics: Condensed Matter*, 22, 2015.

[10] D. G. Rethwisch W. D. Callister. *Materials Science and Engineering 9th Edition, SI Version*. John Wiley and Sons (Asia), 2014.

[11] L. J. Broutman D. Agarwal and K. Chandrashekhara. *Analysis and performance of fiber composites*. John Wiley and Sons, 2017.

[12] A. Maxwell and W. R. Broughton. Survey of long-term durability testing of composites, adhesives and polymers. *National Physical Laboratory*, November 2017.

[13] Ed J. W. Gooch. *Encyclopedic Dictionary of Polymers*. Springer New York, 2007.

[14] T. Bailliez E. Vauthier, J. Abry and A. Chateauminois. Interactions between hygrothermal ageing and fatigue damage in unidirectional glass/epoxy composites. *Composites Science and Technology*, 58(5):687–692, 1998.

[15] R. P. L. Nijssen I. B. C. M. Rocha, F. P. van der Meer and L. J. Sluys. A multiscale and multiphysics numerical framework for modelling of hygrothermal ageing in laminated composites. *Stional Journal for Numerical Methods in Engineering*, 112(4):360–379, 2017.

[16] E. Sideridis and G. Bikakis. Shear properties and load–deflection response of cross–ply glass–epoxy composite short–beams subjected to three-point-bending tests, and the effect of moisture absorption. *Journal of Applied Polymer Science*, 129:2244–2252, 2013.

[17] A. I. Gagani A. E. Krauklis and A. T. Echtermeyer. Hygrothermal aging of amine epoxy: Reversible static and fatigue properties. *Open Engineering*, 8(1):447–454, 2018.

[18] G.C. Papanicolaou and S.P. Zaoutsos. 1 - viscoelastic constitutive modeling of creep and stress relaxation in polymers and polymer matrix composites. In Rui Miranda Guedes, editor, *Creep and Fatigue in Polymer Matrix Composites*, Woodhead Publishing Series in Composites Science and Engineering, pages 3 – 47. Woodhead Publishing, 2011.

[19] J. Bergström. 6 linear viscoelasticity. In *Mechanics of Solid Polymers*, pages 310–350. William Andrew Publishing, 2015.

[20] S. Starkova and A. Aniskevich. Limits of linear viscoelastic behavior of polymers. *Mechanics of Time-Dependent Materials*, 11:111–126, 06 2007.

[21] A. I. Gagani A. E. Krauklis, A. G. Akulichev and A. T. Echtermeyer. Time-temperature-plasticization superposition principle: Predicting creep of a plasticized epoxy. *Polymers*, 11:135–149, 2019.

[22] L. Boltzmann. Zur theorie der elastischen nachwirkung. *Ann. Phys. Chem.*, 7:624–654, 2018.

[23] F. Hoog R.Loy and R. Anderssen. Interconversion of prony series for relaxation and creep. *Journal of Rheology*, 59:1261–1270, 2015.

[24] Christian Bierögel and W. Grellmann. *Fatigue Loading of Plastics - Introduction*, pages 281–286. 01 2014.

[25] Iwan Sahputra and Andreas Echtermeyer. Creep–fatigue relationship in polymer: Molecular dynamics simulations approach. *Macromolecular Theory and Simulations*, 24, 11 2014.

[26] Aifeng Huang, Weixing Yao, and Fang Chen. Analysis of fatigue life of pmma at different frequencies based on a new damage mechanics model. *Mathematical Problems in Engineering*, 2014, 06 2014.

[27] Yong Bai and Wei-Liang Jin. Chapter 28 - spectral fatigue analysis and design. In Yong Bai and Wei-Liang Jin, editors, *Marine Structural Design (Second Edition)*, pages 537 – 556. Butterworth-Heinemann, Oxford, second edition edition, 2016.

[28] Yung-Li Lee and Tana Tjhung. Chapter 3 - rainflow cycle counting techniques. In Yung-Li Lee, Mark E. Barkey, and Hong-Tae Kang, editors, *Metal Fatigue Analysis Handbook*, pages 89 – 114. Butterworth-Heinemann, Boston, 2012.

[29] M. Grieves and J. Vickers. *Digital Twin: Mitigating Unpredictable, Undesirable Emergent Behavior in Complex Systems, in Trans-Disciplinary Perspectives on System Complexity*. Springer Switzerland, 2016.

[30] R. N. Bolton et. al. Customer experience challenges: Bringing together digital, physical and social realms. *Journal of Service Management*, 29(5):776–808, 2018.

[31] R. N. Bolton et. al. Digital twins: The convergence of multimedia technologies. *IEEE Multimedia*, 25(2):87 – 92, 2018.

[32] Subrata Bhowmik. Digital twin of subsea pipelines: Conceptual design integrating iot, machine learning and data analytics. Houston, Texas, 2019. Offshore Technology Conference.

[33] R. E. da Rocha Teixeira. *Fatigue Analysis of Wind Turbine Blades, PHD*. Mechanical Engineering Department Faculty of Engineering of the University of Porto, 2014.

[34] J. Rinker. Rainflow counting in python - cycle counts and ranges with/without goodman correction. `https://gist.github.com/jennirinker/688a917ccb7a9c14e78f`, 2015.

[35] Zongjin Lu, Bill Feng, and Charlie Loh. Fatigue behaviour and mean stress effect of thermoplastic polymers and composites. *Frattura ed Integrita Strutturale*, 12:150–157, 10 2018.

[36] Ivan Saprunov, Marina Gergesova, and Igor Emri. Prediction of viscoelastic material functions from constant stress- or strain-rate experiments. *Mechanics of Time-Dependent Materials*, 18, 05 2013.

[37] P. Janiszewski. Implementation of astm e1049-85 rainflow cycle counting algorithm. `https://github.com/iamlikeme/rainflow/`.

Appendix

Python files are added with the report as a .zip file. Short description of what each file does follows:

digitalTwinComplete - The complete digital twin, where corresponding lists of stress, time, temperature, conditioning levels are entered. The output is the resulting creep and fatigue damage

stressStrainCurve - Calculates $\sigma - \varepsilon$ for a constant strain-rate, as a function of temperature and moisture level

multiprocessing - An example of how multiprocessing can be implemented, in this case for plotting how creep develops as a function of time.

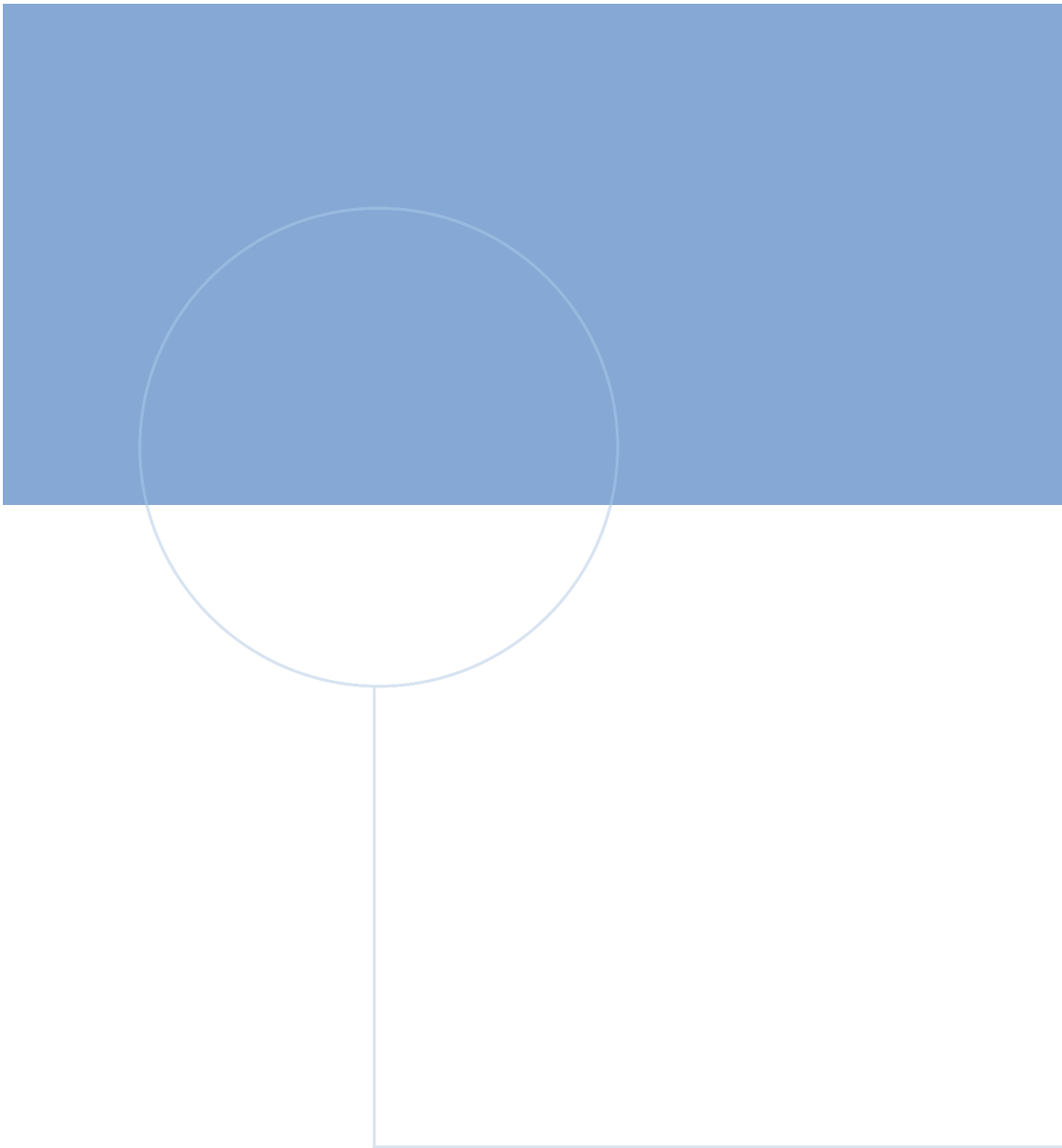

NTNU

Norwegian University of
Science and Technology